

Appearance of the octupole ordered phase IV in $\text{Ce}_x\text{La}_{1-x}\text{B}_6$

M. Sera,¹ K. Kunimori,¹ T. Matsumura,¹ A. Kondo,² H. Tanida,³ H. Tou,⁴ and F. Iga⁵

¹*Department of ADSM, Hiroshima University, Higashi-Hiroshima 739-8530, Japan*

²*Institute for Solid State Physics, The University of Tokyo, Kashiwa, Chiba 277-8581, Japan*

³*Department of Intelligent System Design Engineering, Faculty of Engineering, Toyama Prefectural University, Imizu, Toyama 939-0398, Japan*

⁴*Department of Physics, Graduate School of Science, Kobe University, Kobe 657-8501, Japan*

⁵*College of Science, Ibaraki University, Mito 310-0398, Japan*



(Received 2 November 2017; revised manuscript received 15 February 2018; published 14 May 2018)

We investigated the physical properties of $\text{Ce}_x\text{La}_{1-x}\text{B}_6$ at $x \sim 0.8$, below which the T_β -type antiferro-octupole (AFO) ordered phase IV appears as a result of the larger suppression rate of T_Q than T_N by La doping. The most important result is that while the peak of the specific heat at T_Q is rapidly suppressed and broadened by La doping, that at T_{IV} is sharp and large. This indicates that although the T_β -AFO order in the phase IV is robust against the local lattice distortion induced by La doping, the O_{xy} -type antiferroquadrupole (AFQ) ordered phase II is very weak. The T_{xyz} -AFO interaction is robust against La doping from the observation of the pronounced enhancement of T_Q even in a small x region. Based on these La-doping effect of the multipole interactions, we carried out the mean-field calculation for the four-sublattice model to reproduce the magnetic phase diagrams of $\text{Ce}_x\text{La}_{1-x}\text{B}_6$. Based on the calculated results, we propose that the small splitting of the quartet is induced by La doping in phase I to explain the magnetic phase diagram for $x < 0.65$. We could obtain the calculated results roughly consistent with the experimental results, although there appear new problems. We classified the mechanisms of the four different types of the competition among the four interactions with roughly the same magnitude, which induce the interesting and complicated properties in $\text{Ce}_x\text{La}_{1-x}\text{B}_6$.

DOI: [10.1103/PhysRevB.97.184417](https://doi.org/10.1103/PhysRevB.97.184417)

I. INTRODUCTION

The multipole order is one of the topics of the f -electron systems [1–3]. Different from the magnetic order, the multipole order is difficult to observe directly by the microscopic measurements such as a neutron diffraction. Such a multipole order is often called as a hidden order. By the progress of the resonant x-ray-diffraction experiments, the direct observation of the multipole order has been possible.

$\text{Ce}_x\text{La}_{1-x}\text{B}_6$ is one of the most famous compounds exhibiting unusual multipole orders. Figures 1(a) and 1(b) show the schematic pictures of the magnetic phase diagrams of CeB_6 and $\text{Ce}_{0.7}\text{La}_{0.3}\text{B}_6$, respectively, and Fig. 1(c) shows the x dependence of the transition temperatures of $\text{Ce}_x\text{La}_{1-x}\text{B}_6$ [4–26]. Three phases exist in CeB_6 : phase I is paramagnetic, phase II is the O_{xy} -type antiferroquadrupole (AFQ) ordered phase, phase III is the $2\text{-}k\text{-}k'$ antiferromagnetic (AFM) ordered phase. The I-II phase boundary T_Q is unusually enhanced by magnetic field. The magnetic phase diagram of $\text{Ce}_{0.7}\text{La}_{0.3}\text{B}_6$ is also unusual; phase IV exists at low magnetic fields and phases III and II are shifted towards higher magnetic fields. As for the x dependence of the transition temperatures, T_Q and T_N are suppressed by La doping as is seen in Fig. 1(c). Since the suppression rate of T_Q is larger than that of T_N , these two transition temperatures seem to coincide with each other at $x \sim 0.8$. For $x < 0.8$, phase II disappears and phase IV appears. Recently, it was reported that the above x dependence of the transition temperatures at $x \sim 0.8$ is not correct [3] which will be discussed later.

At the early stage, the detailed nature of phase II was not known and extensive studies were performed to clarify the microscopic nature of this phase. At the early stage, the crystalline electric-field (CEF) level scheme was not correct. This also made the clarification of phase II difficult [5,27]. In phase II, the long-range order (LRO) could not be observed by the neutron diffraction at $H = 0$. However, by the NMR and neutron-diffraction experiments, it was discovered that the antiferromagnetic moment (M_{AF}) component is induced by magnetic field and the results were understood as the AFQ order [28–30]. However, there remained the discrepancy in the understanding of the results between the neutron diffraction and NMR. The former indicated single $\mathbf{k} = [\frac{1}{2}\frac{1}{2}\frac{1}{2}]$ order [29,30] and the latter was analyzed by assuming triple- \mathbf{k} order [28]. Theoretically, Hanzawa and Ohkawa proposed the AFQ or the orbital order. Hanzawa proposed AFQ order with the Γ_7 doublet ground state and could reproduce the enhancement of T_Q with magnetic field [31,32]. Hanzawa's model is, in some sense, similar to the singlet ground-state problem exhibiting magnetic or quadrupole order through the excited states [33–36]. However, the CEF ground state was found to be the Γ_8 quartet by the inelastic neutron scattering, etc. [37,38]. Ohkawa, assuming the Γ_8 ground state correctly, first pointed out the essential importance of the higher-order interaction originating from the spin and orbital degeneracies, by which T_Q is enhanced by magnetic field [39,40]. Shiina *et al.* showed more rigorously that the octupole interaction plays an essential role in phase II [41,42]. While the magnetic field induced M_{AF} was discussed by Hanzawa and Ohkawa,

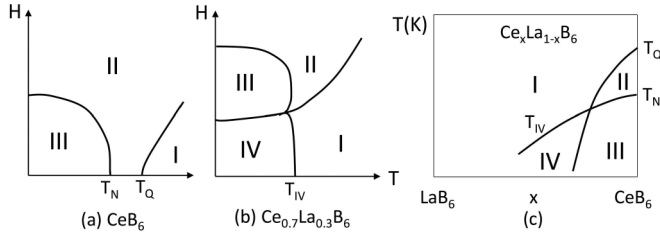


FIG. 1. Schematic pictures of magnetic phase diagram of (a) CeB_6 and (b) $\text{Ce}_{0.7}\text{La}_{0.3}\text{B}_6$, (c) x dependence of the transition temperatures of T_Q , T_N , and T_{IV} in $\text{Ce}_x\text{La}_{1-x}\text{B}_6$ at $H = 0$.

the details of the relation between the applied magnetic field and the direction of M_{AF} were not discussed. Here, we note the following: (1) Rossat-Mignod pointed out that the sixth order in the exchange interaction is necessary to construct the $2\text{-}k\text{-}k'$ AFM structure in phase III [30]; (2) Erkelens *et al.* observed that $M_{AF} \parallel [001]$ is induced by $H \parallel [110]$ and proposed the O_{yz} or O_{zx} AFQ order [43].

Sakai *et al.* explained the discrepancy of the ordering vector between neutron diffraction and NMR by the coexistence of the O_{xy} -type AFQ order and the T_{xyz} -type antiferro-octupole (AFO) order [44,45]. Thus, the importance of the higher-order multipole interactions was revealed. These were confirmed by the resonant x-ray-scattering experiments [46,47]. By assuming the O_{xy} -type AFQ order and introducing the T_{xyz} -type AFO interaction, many of the characteristic properties of both phases of III and II could be explained by the mean-field calculation for the four-sublattice model in which the T_{xyz} -type AFO interaction coexists with O_{xy} -type AFQ and AFM interactions [48–50]. The fluctuation effect induced by the multipole interactions was also investigated both experimentally and theoretically [51–55].

In the course of the studies of $\text{Ce}_x\text{La}_{1-x}\text{B}_6$, phase IV was discovered. This phase exhibits the following characteristic properties: a peak of χ at T_{IV} [15,16]; a large peak of the specific heat at T_{IV} accompanied with a large magnetic entropy [21,24]; a large softening of the elastic constant C_{44} ; no magnetic order [56–60]. Kubo and Kuramoto proposed the T_β -type AFO order which could explain the above characteristic properties consistently [61,62]. This T_β -type AFO order was verified by the resonant x-ray- and neutron-diffraction experiments [63–66].

The interesting properties in $\text{Ce}_x\text{La}_{1-x}\text{B}_6$ were induced by the coexistence and competition among the four different kinds of interaction, i.e., O_{xy} AFQ, T_{xyz} AFO, AFM, and T_β AFO, with roughly the same magnitude. Generally, the Ce-Ce interaction is reduced by La doping in Ce compounds. Nevertheless, in the present system, the T_β AFO interaction whose existence could not be recognized in CeB_6 plays the essential role for $x < 0.8$. This indicates that the x dependencies of the four interactions are different. (1) The first purpose in the present paper is to clarify how phase IV appears at $x \sim 0.8$ and the details of the competition between the T_β AFO interaction and the other three interactions experimentally and we performed the detailed experimental studies focused on the $x \sim 0.8$ region. The physical properties of CeB_6 and phase IV themselves were investigated in detail by the mean-field approximation [48,61,62]. However, the effect on phase IV by

the other three interactions have not been studied in detail. (2) The second purpose is to clarify the mechanism of the competition between T_β AFO and the other three interactions within the framework of the mean-field approximation and we performed the mean-field calculation for the four sublattice model with the four different types of interactions.

II. EXPERIMENT

Single crystals of $\text{Ce}_x\text{La}_{1-x}\text{B}_6$ ($x = 0.82, 0.8, 0.75, 0.7, 0.6$) were prepared by a floating zone method. The specific heat was measured by using a physical property measurement system (PPMS) above $T = 0.4$ K. The magnetization was measured by the superconducting quantum interference device (SQUID) magnet meter [magnetic property measurement system (MPMS)] down to 1.8 K and below 5 T at the ambient pressure and was measured by the home-made extraction method down to 1.4 K and under pressure up to 1 GPa. The electrical resistivity was measured by the usual ac four-probe method in magnetic field up to 14.5 T and down to 0.4 K using a ^3He refrigerator.

III. EXPERIMENTAL RESULTS

A. Specific heat of $\text{Ce}_x\text{La}_{1-x}\text{B}_6$

The temperature (T) dependencies of the specific heat (C) of $\text{Ce}_x\text{La}_{1-x}\text{B}_6$ in zero magnetic field are shown in Fig. 2(a). In CeB_6 , a peak of C is sharp both at $T_Q = 3.3$ K and $T_N = 2.3$ K. A peak height at T_Q is much smaller than that expected from the splitting of the Γ_8 quartet. This is due to the large short-range-order (SRO) effect above T_Q . A peak at T_Q is rapidly suppressed by La doping. For $x = 0.85$, although a sharp peak is observed at $T_N = 1.9$ K, only a broad shoulder appears at $T_Q = 2.2$ K. For $x = 0.82$, although only one sharp peak is observed at $T_N = 1.8$ K at first sight, T_Q at $H = 0$ exists a little above T_N at $H = 0$, which will be shown later. For $x = 0.8$, two rather sharp peaks are observed at $T_N = 1.6$ K and $T_{IV} = 1.7$ K. Thus, while phase II disappears at $x \sim 0.81$, in place, phase IV appears for $x < 0.8$. For $x = 0.75$, a sharp peak is observed at $T_{IV} = 1.6$ K and a tiny peak at $T_N = 1.1$ K. For $x = 0.7$, only one sharp peak is observed at $T_{IV} = 1.4$ K. For $x = 0.6$, a peak at $T_{IV} = 0.93$ K is very broad due to a much larger amount of La doping.

The T dependencies of C of $\text{Ce}_{0.82}\text{La}_{0.18}\text{B}_6$ for $H \parallel [001]$ are shown in Fig. 2(b). While a sharp peak is observed at $T_N = 1.8$ K, the anomaly at T_Q is almost impossible to recognize at $H = 0$. However, by applying magnetic field of $H = 0.1$ T, a small shoulder appears at $T_Q \sim 2.0$ K and is enhanced with increasing magnetic field.

The T dependencies of C of $\text{Ce}_{0.8}\text{La}_{0.2}\text{B}_6$ for $H \parallel [110]$ are shown in Fig. 2(c). Although at $H = 0$, the two peaks are observed at $T_N = 1.6$ K and $T_{IV} = 1.7$ K, at $H = 0.6$ T, T_{IV} disappears and a very sharp peak and a broad one are observed at $T_N = 1.65$ K and $T_Q \sim 2$ K, respectively. At $H = 1.2$ T, the three peaks are observed at $T_{N2} \sim 1.4$ K, $T_N \sim 1.55$ K, and $T_Q \sim 2.5$ K. T_{N2} originates from the transition inside phase III. At $H = 2$ T, the two sharp peaks at $T_N \sim 1.3$ K and $T_Q \sim 3$ K are observed. Here, we note that a peak at T_N is small for $H < 0.4$ T where $T_N < T_{IV}$ and is large and sharp for $x > 0.6$ T where $T_N < T_Q$.

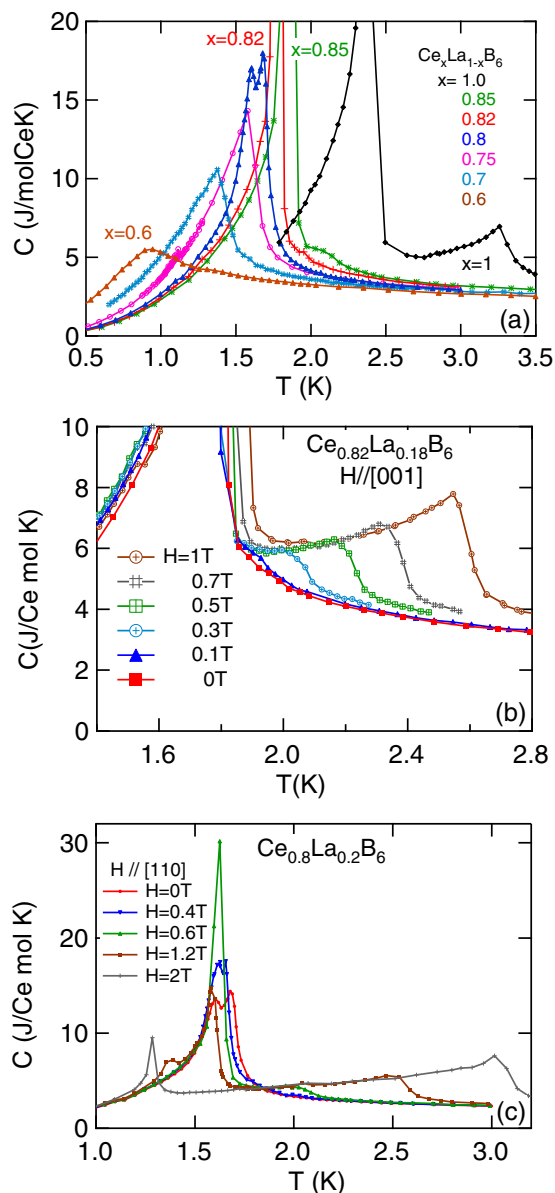


FIG. 2. Temperature dependencies of the specific heat (C) of $Ce_xLa_{1-x}B_6$ in zero magnetic field, (b) $Ce_{0.82}La_{0.18}B_6$ for $H \parallel [001]$, and (c) $Ce_{0.8}La_{0.2}B_6$ for $H \parallel [110]$. In (a), the result of CeB_6 is cited from Ref. [17] and $T_Q = (2.3, 1.90, 1.79)$ K and the magnitude of C at $T_Q = (33, 44, 55)$ J/mol CeK for $x = 1, 0.85,$ and 0.82 , respectively.

B. Magnetic and transport properties of $Ce_xLa_{1-x}B_6$

Figures 3(a)–3(d) show the T dependencies of the magnetization (M) of $Ce_xLa_{1-x}B_6$ ($x = 0.85, 0.82, 0.8, 0.75$) at low magnetic fields, respectively. For $x = 0.85$, M exhibits an increase below T_Q and a decrease below T_N . The anomalies at T_Q and T_N are enhanced by magnetic field. For $x = 0.82$, an increase is observed below T_Q , which is enhanced with increasing magnetic field. For $x = 0.8$, T_{IV} at which a peak is observed appears and exists up to 0.3 T. Above 0.4 T, T_Q appears in place of T_{IV} . A large enhancement is observed below T_N . For $x = 0.75$, only one transition is observed at T_{IV} below 0.4 T. Above this field, T_N appears and it is enhanced by magnetic field. Above 0.7 T, T_Q appears, which is considerably

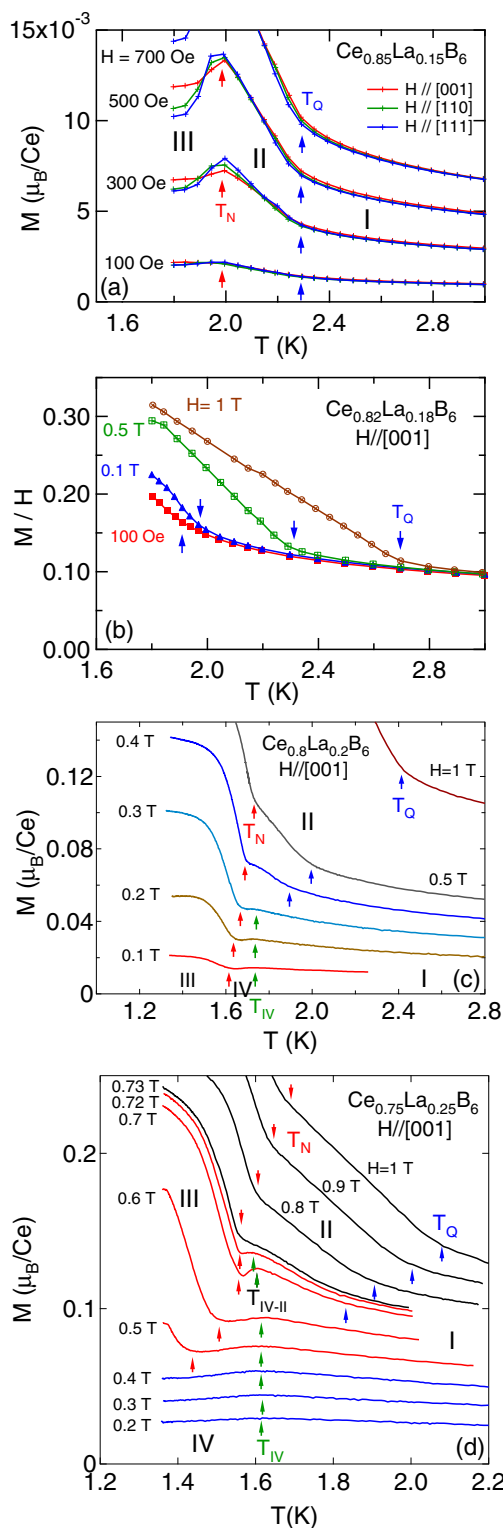


FIG. 3. Temperature dependencies of magnetization of (a) $Ce_{0.85}La_{0.15}B_6$ for $H \parallel [001]$, $[110]$, and $[111]$, (b) $Ce_{0.82}La_{0.18}B_6$ for $H \parallel [001]$, (c) $Ce_{0.8}La_{0.2}B_6$ for $H \parallel [001]$, and (d) $Ce_{0.75}La_{0.25}B_6$ for $H \parallel [001]$.

enhanced with increasing magnetic field. It is noted that in a narrow field region between 0.7 and 0.72 T, the successive transitions $III \leftarrow IV \leftarrow II \leftarrow I$ are observed.

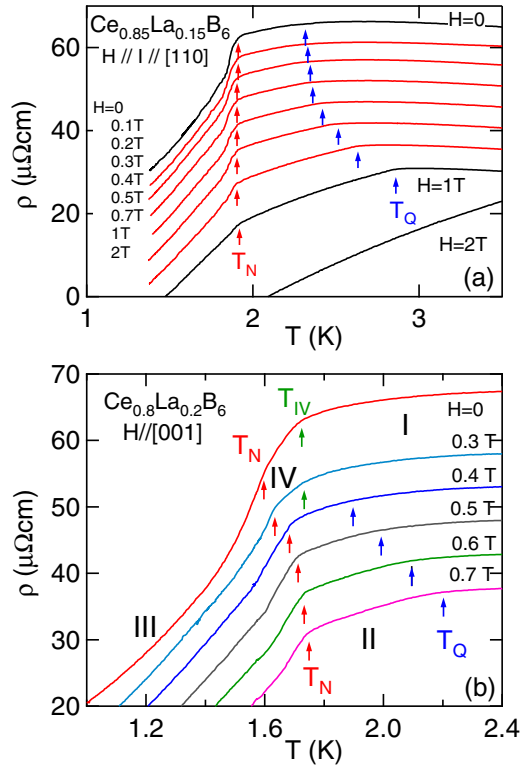


FIG. 4. Temperature dependencies of the electrical resistivity of (a) $\text{Ce}_{0.85}\text{La}_{0.15}\text{B}_6$ for $H \parallel [110]$ and (b) $\text{Ce}_{0.8}\text{La}_{0.2}\text{B}_6$ for $H \parallel [001]$.

Figures 4(a) and 4(b) show the T dependencies of the electrical resistivity (ρ) of $\text{Ce}_x\text{La}_{1-x}\text{B}_6$ ($x = 0.85, 0.8$), respectively. For $x = 0.85$, although a kink at T_Q is clearly observed at high magnetic fields, it is quite difficult to recognize below 0.1 T, indicating the very small splitting of the Γ_8 quartet at low magnetic fields in phase II. On the other hand, the decrease of ρ below T_N is clearly observed, due to the large splitting of the energy levels below T_Q . For $x = 0.8$, the two transitions are recognized at T_N and T_{IV} . At $H = 0.4$ T, T_{IV} disappears and only one step decrease is observed below T_N . At $H = 0.5$ T, the two anomalies are observed at T_N and T_Q .

C. Magnetic phase diagrams and x dependencies of transition temperatures of $\text{Ce}_x\text{La}_{1-x}\text{B}_6$

Figure 5 shows the magnetic phase diagrams of $\text{Ce}_x\text{La}_{1-x}\text{B}_6$ obtained from the present results. With decreasing x , T_Q approaches T_N due to the larger suppression rate of T_Q by La doping. However, just before $T_Q = T_N$ is realized, phase IV appears at low magnetic fields. Once phase IV appears, the region of phase IV expands rapidly towards the low-temperature region with decreasing x . Above $H \sim 1$ T, the successive phase transition of $I \rightarrow II \rightarrow III$ takes place from the higher temperature side, independent of x . However, in the low magnetic field region, a drastic change appears due to the appearance of phase IV. The H dependence of T_Q at low magnetic fields is changed below and above $x \sim 0.81$. For $x > 0.82$, it is convex. On the other hand, for $x < 0.8$, it is concave. These suggest that although the $I \rightarrow II$ transition appears easily for $x > 0.82$, it is difficult when phase IV exists at low magnetic fields. We note that for $x > 0.82$, although

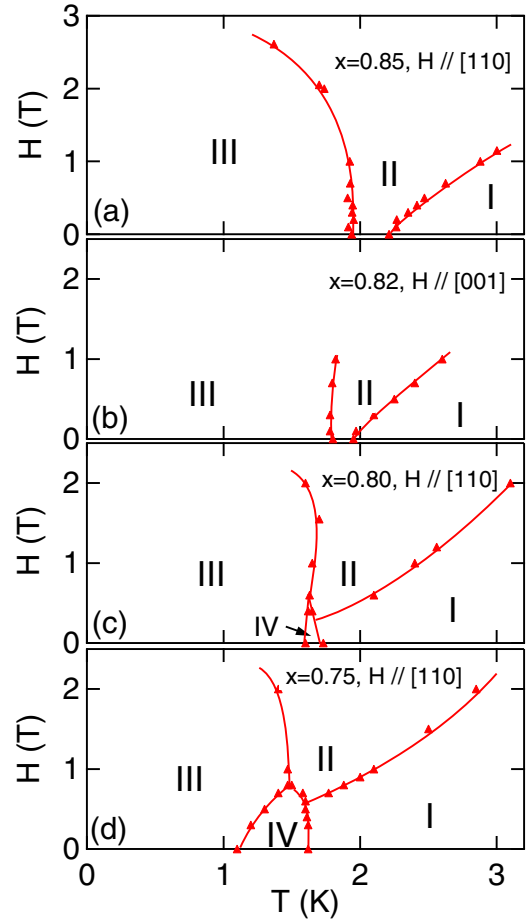


FIG. 5. Magnetic phase diagrams of $\text{Ce}_x\text{La}_{1-x}\text{B}_6$ for (a) $x = 0.85$, (b) $x = 0.82$, (c) $x = 0.8$, and (d) $x = 0.75$. For $x = 0.85, 0.8$, and 0.75 $H \parallel [110]$ and for $x = 0.82$, $H \parallel [001]$.

the $I \rightarrow II$ transition is very sharp at high magnetic fields as in CeB_6 , it is very weak and broad at low fields below ~ 0.1 T. We also note that the II-IV transition exists at finite magnetic fields for $x = 0.8$ and 0.75 as if it appears to avoid the direct transition from phase I to III.

Figure 6 shows the x dependencies of the transition temperatures, T_Q , T_N , and T_{IV} of $\text{Ce}_x\text{La}_{1-x}\text{B}_6$ at $H = 0$. Previously, although the continuous x dependence of T_N and T_{IV} through $x \sim 0.8$ was reported, as if there exists the quadruple-critical point [16,19,22], the present results deny the existence of the quadruple-critical point as was recently reported by Cameron *et al.* [3]. In the inset of Fig. 6(a), the conjectured x dependencies of the transition temperatures at $x \sim 0.81$ at $H = 0$ are shown. The direct $I \rightarrow III$ transition does not exist but another phase of IV or II exists between I and III independent of the x value, which is drawn by a black solid line. The negative slope of the $II \rightarrow IV$ phase boundary, which is shown in the inset of Fig. 6(a), is expected from the successive phase transitions of $I \rightarrow II \rightarrow IV \rightarrow III$ as observed from the higher temperature side at $H \sim 0.7$ T in $\text{Ce}_{0.75}\text{La}_{0.25}\text{B}_6$ in Fig. 3(d). Since the $I \rightarrow II$ and $I \rightarrow IV$ phase transitions are of second order, the $II \rightarrow IV$ transition is expected to be first order. However, this is not clear at present because only a broad peak is seen at T_{IV-II} in the $M-T$ curve, which could be due to the

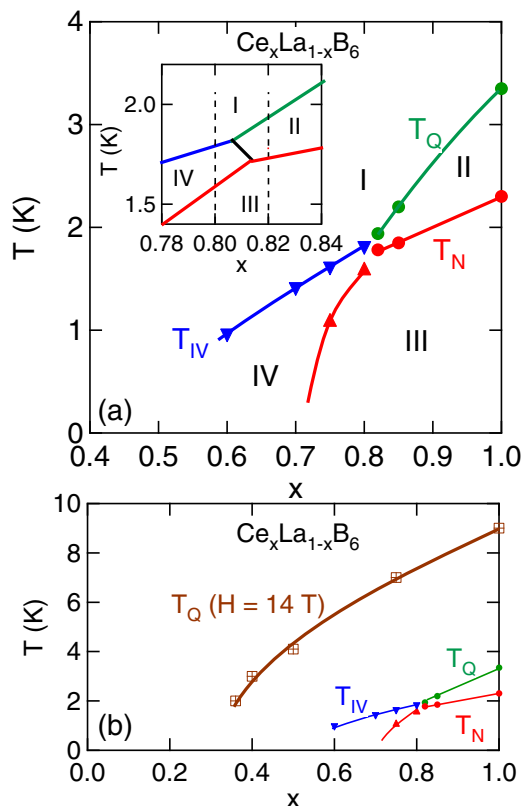


FIG. 6. x dependence of the transition temperatures (T_Q , T_N , T_{IV}) of $Ce_xLa_{1-x}B_6$ (a) at $H = 0$. The inset shows the conjectured x dependence of the transition temperatures around $x \sim 0.81$ at $H = 0$. (b) x dependence of T_Q at $H = 14$ T cited from [22].

randomness effect induced by La doping. At high magnetic fields, the T_{xyz} -type AFO interaction enhances the O_{xy} -type AFQ interaction. Although T_Q at $H = 0$ is rapidly suppressed with decreasing x , T_Q at $H = 14$ T remains down to $x \sim 0.3$.

IV. DISCUSSION

A. x dependencies of the O_{xy} -AFQ, T_{xyz} -AFO, AFM, and T_β -AFO interactions in $Ce_xLa_{1-x}B_6$ and appearance of phase IV

First, we discuss the origin of the different La-doping effect on the multipole interactions in $Ce_xLa_{1-x}B_6$. The suppression of the transition temperatures by La doping exhibits the different behaviors. It is large for T_Q but is small for T_N and T_{IV} . The La-doping effect on the peak shape of C at the transition temperatures is also different. That of C at T_Q is rapidly suppressed and is broadened by La doping. On the other hand, that at T_{IV} remains sharp and large at least down to $x = 0.7$, nevertheless $x = 0.7$ is much smaller than $x = 0.82$. Namely, phase IV is robust against La doping and T_{IV} is not distributed, but phase II is very weak and T_Q is distributed significantly. This suggests that although the perpendicular alignment of the anisotropic O_{xy} -quadrupole moment in phase II is easily destroyed by the local lattice distortion induced by La doping, the ferroalignment of the $O_{xy} + O_{yz} + O_{zx}$ -quadrupole moment accompanied with the T_β -type AFO order in phase IV [61,62] is robust against the local disturbance although the $O_{xy} + O_{yz} + O_{zx}$ -quadrupole

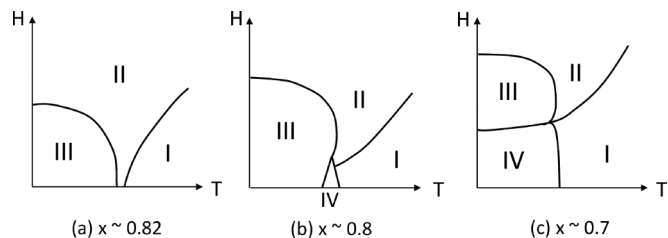


FIG. 7. Schematic pictures of the magnetic phase diagrams of $Ce_xLa_{1-x}B_6$: (a) $x \sim 0.82$, (b) $x \sim 0.8$, and (c) $x \sim 0.7$.

moment is anisotropic. Due to the large randomness effect induced by La doping, T_Q is distributed significantly. This leads to the broad peak of C at T_Q . The T_{xyz} -type AFO interaction, which plays an important role in magnetic fields, is also robust against La doping regardless of the AFO order as is seen in Fig. 6(b). The pronounced enhancement of T_Q by magnetic field observed even in a small x region down to 0.37 [20] also supports the robustness of the T_{xyz} -AFO interaction against La doping. This is because the T_{xyz} -octupole moment is rather spherical as is seen from $T_{xyz} \propto \overline{J_x J_y J_z}$. The AFM exchange interaction is also strong against La doping because this interaction is isotropic, in principle. Thus, as for the different suppression rate of the transition temperatures by La doping, there seems to exist the following tendency. Although the ferromultipole order and the AF-multipole order by rather spherical multipole moment are robust against the local lattice disturbance induced by La doping, the AF-multipole order by the anisotropic multipole moment is weak against the local disturbance. If the AFM order appears in place of phase IV in $Ce_xLa_{1-x}B_6$, the collinear AFM structure might be realized. However, experiments show that not the collinear AFM order but the phase IV appears at $x \sim 0.8$. This is consistent with the expectation of $T_{IV} > T_N$ as is suggested in Fig. 6(a).

The magnetic phase diagram of $Ce_xLa_{1-x}B_6$ is drastically changed below $x \sim 0.8$ as is shown in Fig. 7. Once phase IV appears, phase II is shifted towards the higher magnetic fields. For $x = 0.7$, both phases III and II exist only at the finite magnetic fields. At $x \sim 0.8$ where phase IV appears, the magnitudes of the four interactions should be roughly the same and the competition among these interactions should be complicated. To understand the results of $Ce_xLa_{1-x}B_6$, the x dependence of the O_{xy} -AFQ, T_{xyz} -AFO, AFM, and T_β -AFO interactions should be known and how these interactions work cooperatively or compete with each other should be clarified.

B. Mean-field calculation for the four-sublattice model to reproduce the magnetic phase diagrams of $Ce_xLa_{1-x}B_6$

To obtain the information on the competition among the four different interactions, we carried out the mean-field calculation for the four-sublattice model that includes the four interactions of the O_{xy} -AFQ, T_{xyz} -AFO, AFM, and T_β -AFO. The randomness effect induced by La doping could not be taken into account. We use the bare transition temperatures of T_Q^0 , T_{xyz}^0 , T_N^0 , and T_b^0 when we discuss the magnitude of the O_{xy} -AFQ, T_{xyz} -AFO, AFM, and T_β -AFO interactions. T_Q^0 means the O_{xy} -AFQ temperature when the O_{xy} -AFQ interaction exists independently. To calculate the magnetic phase diagrams of

$\text{Ce}_x\text{La}_{1-x}\text{B}_6$, it is necessary to know the x dependence of these four interactions. For $x > 0.82$, it is not easy to determine the appropriate magnitudes of the interactions because T_Q^0 and T_N^0 are known from the experiments. However, for $x < 0.8$, it is difficult because the transition temperature to phase IV is the highest, where the ground state of phase IV is nonmagnetic singlet. Thereby, we investigated the details of the magnitude relation under the various conditions and based on these results, we determined the magnitudes of T_Q^0 , T_{xyz}^0 , T_N^0 , and T_b^0 for $x < 0.8$. Those used in the calculation are shown in Fig. 14. The details are shown in the Appendix. The obtained magnetic phase diagrams are shown in Figs. 16(a)–16(d). The characteristics of the magnetic phase diagrams could be reproduced by the calculation, although there remain several problems to be solved.

For $x > 0.82$, the calculated results are consistent with the experimental results rather well, as will be shown in Fig. 16(a). This is because the O_{xy} -AFQ and T_{xyz} -AFO interaction work cooperatively and the AFM interaction is compatible with the O_{xy} -AFQ order, when T_Q is larger than T_N .

For $x < 0.8$, the T_β -AFO interaction with the nonmagnetic singlet ground state plays an important role and competes with the AFM and O_{xy} -AFQ interactions with the magnetic ground state. This leads to the complicated competitions among the four interactions. However, the magnetic phase diagrams similar to the experimental results could be reproduced for $x < 0.8$. For $x = 0.8$ and 0.75, phase IV appears above T_N at $H = 0$ and phases III and II in magnetic fields are consistent with the experimental results, as will be shown in Figs. 16(b) and 16(c), respectively. For $x = 0.7$, the ground state at low magnetic fields is phase IV and phase III appears in finite magnetic fields inside phase II, as will be shown in Fig. 16(d).

In the present calculation, we find the four different types of the competition play an important role in $\text{Ce}_x\text{La}_{1-x}\text{B}_6$: the competition (1) between the O_{xy} -AFQ order and the $O_{xy} + O_{yz} + O_{zx}$ -FQ order accompanied with the T_β -AFO order [67], and (2) between the AFM and FM orders (the latter originates from the coexistence of the O_{xy} -AFQ and T_{xyz} -AFO orders), (3) between the magnetic (phase III) and nonmagnetic (phase IV) ground states, and (4) between the magnetic anisotropy, i.e., the easy axis along the fourfold axis and the twofold one. The former originates from the CEF effect and the latter from the coexistence of the O_{xy} -type, T_{xyz} -AFO, and AF exchange interactions. These four different types of the competition make the ground state in $\text{Ce}_x\text{La}_{1-x}\text{B}_6$ very complicated.

C. Remaining problems

The calculated magnetic phase diagrams are roughly consistent with the experimental results. However, there appear the following problems. (1) Although for $x = 0.8$ and 0.75, the AFM order is obtained as the ground state at $H = 0$, this is not phase III in which the noncollinear AFM order with spins along the twofold axis is realized. The calculated results show the AFM order with the antiferrocomponent along the z axis or that with spins along the fourfold axis. (2) A peak of the magnetic susceptibility at T_{IV} could not be reproduced, as will be shown in Fig. 18(b). (3) Although the $IV \leftarrow II$ transition in magnetic fields is observed for $x = 0.8$ and 0.75 as is shown in

Figs. 5(c) and 5(d), the calculation could not reproduce this type of transition. In the calculation under the condition of $T_b^0 < T_Q^0$, although the $II \rightarrow IV$ transition from the higher temperature side appears at $H = 0$, this transition disappears once the magnetic field is applied as will be shown in Fig. 9(f-1). In the calculation, the successive phase transitions of $I \rightarrow IV \rightarrow II \rightarrow III$ from the higher temperature side is obtained as will be shown in Figs. 16(b) and 16(c). This contradicts the experimental results in Figs. 5(c) and 5(d). (4) For $x = 0.7$, T_N in finite magnetic field inside the phase II is much smaller than T_b^0 at $H = 0$ T. This originates from the rapid suppression of T_Q under the T_β -AFO order, as will be shown in Fig. 12. However, this contradicts the experimental results where these two transition temperatures are nearly the same as is seen in Fig. 7(c). (5) When the magnitudes of T_Q^0 and T_{xyz}^0 are close to each other, which is realized for $x > 0.8$, the pronounced enhancement of the I-II transition temperature in magnetic field is obtained as is seen in the experiments. However, with decreasing x below 0.8, T_Q is rapidly suppressed. This leads to the rapid suppression of the ratio of T_Q^0/T_{xyz}^0 in the calculation. Then, the enhancement of the I-II transition temperature in magnetic fields is reduced rapidly with decreasing x and is expected to disappear for $x < 0.65$ because the O_{xy} -AFQ and T_{xyz} -AFO interactions do not coexist in this x region as is seen in Fig. 15. These contradict the experimental results, where even for $x = 0.37$, the clear enhancement of T_Q is observed in magnetic fields [20]. To explain this discrepancy, we propose that the CEF splitting could appear with decreasing x . The La doping breaks the cubic symmetry around the Ce ion and the fourfold degeneracies of the Γ_8 quartet might be lifted and the magnitude of its splitting might increase with decreasing x at $H = 0$. This splitting rapidly suppresses the O_{xy} -type AFQ interaction in phase I as in the case of the magnetic order in the system with the singlet ground state. Such a splitting of the quartet fourfold degeneracies was suggested in the softening of C_{66} of $\text{Ce}_{0.5}\text{La}_{0.5}\text{B}_6$ in phase I by magnetic field [68–70]. In the phase I of CeB_6 , both C_{44} and C_{66} modes show the hardening by magnetic field as usual. However, in phase I in $\text{Ce}_{0.5}\text{La}_{0.5}\text{B}_6$, although C_{44} shows a hardening, C_{66} shows a softening by magnetic field. This softening is difficult to expect in the fourfold degenerated CEF ground state and suggests the small splitting of the quartet in the paramagnetic region. This is supported by the present calculation whose details will be shown in the Appendix (Secs. 5 and 6). The details of the proposed splitting of the Γ_8 quartet in phase I by La doping are not known at present.

V. CONCLUSION

We performed the detailed investigations of the thermal, magnetic, and transport properties of $\text{Ce}_x\text{La}_{1-x}\text{B}_6$ at $x \sim 0.8$, below which the T_β -type AFO ordered phase IV appears. While the peak of the specific heat at T_Q at $H = 0$ is rapidly suppressed and broadened by La doping, that at T_{IV} is sharp and large. This indicates that although the T_β -type AFO order in phase IV is robust against the local lattice distortion induced by La doping, the O_{xy} -type AFQ ordered phase II is very weak. The T_β -AFO interaction is also robust against La doping from the pronounced enhancement of T_Q by magnetic field even in

a small x region. For $x = 0.82$ just above 0.8 where phase IV appears, a peak of C at $H = 0$ is scarcely recognized at T_Q , while that at T_N is very sharp and large. Phase IV appears when T_Q is reduced and the O_{xy} -AFQ order is weakened very much at $H = 0$ by La doping. However, once the magnetic field is applied, the O_{xy} -AFQ order revives rapidly even when T_Q is scarcely recognized at $H = 0$.

Based on these La-doping dependencies of the multipole interactions, we tried to reproduce the magnetic phase diagrams of $\text{Ce}_x\text{La}_{1-x}\text{B}_6$ by the mean-field calculation for the four-sublattice model, although the randomness effect by La doping could not be taken into account. The calculated magnetic phase diagrams are roughly consistent with the experimental results. In order that phase III appears for $X < 0.8$, not the AFM interaction but the O_{xy} -AFQ one, plays the dominant role. The details of the effect on phase IV by the other three interactions were revealed within the framework of the mean-field approximation as follows: the competition between (1) O_{xy} -AFQ order and $O_{xy} + O_{yz} + O_{zx}$ -FQ order accompanied by the T_β -AFO order, (2) AFM order and FM order induced by the coexistence of the O_{xy} -AFQ and T_{xyz} -AFO order, (3) magnetic ground state in phase III and nonmagnetic ground state in phase IV, and (4) magnetic easy axis along the fourfold axis by the CEF effect and along the twofold axis induced by the coexistence of the O_{xy} -AFQ, T_{xyz} -AFO, and AFM orders. On the other hand, the following problem was found to appear in the present calculation. The enhancement of T_Q by magnetic field could not be obtained for $x < 0.65$, because the O_{xy} -AFQ and T_{xyz} -AFO orders do not coexist due to the disappearance of T_Q at $H = 0$. This contradicts the experimental results. To avoid this discrepancy, we propose the small splitting of the Γ_8 quartet by La doping, as one possibility, in which the magnetic field could induce the O_{xy} -AFQ order. In the mean-field calculation, a peak of C at T_Q is sharp and large independent of the x value. This contradicts the experimental results. To explain the experimental results, it is necessary to take the SRO effect and the local disturbance induced by the La doping into account. Further theoretical investigations are necessary to reveal their details, in the future.

ACKNOWLEDGMENTS

The authors would like to thank Professor Y. Kuramoto and Professor R. Shiina for stimulating discussions. One of the authors (M.S.) would like to express sincere thanks to Dr. J. Rossat-Mignod who led him in the CeB_6 physics. This work was supported by JSPS Grant Aid for Scientific Research (c) No. 15K05173.

APPENDIX

We have carried out the mean-field calculation for the four-sublattice model in which the CEF potential with the Γ_8 - Γ_7 splitting of 540 K, for the O_{xy} -AFQ, T_{xyz} -AFO, T_β -AFO, and AF exchange interactions, is taken into account. Here, $T_\beta = (T_\beta^x + T_\beta^y + T_\beta^z)/\sqrt{3}$ as was proposed by Kuramoto *et al.* It is known that the ordering vector of the O_{xy} -AFQ, T_{xyz} -AFO, and T_β -AFO order is the same, i.e., $\mathbf{k} = [\frac{1}{2}\frac{1}{2}\frac{1}{2}]$. We note that the randomness effect induced by La doping and also the SRO

effect by the multipole could not be taken into account in the recent mean field calculation. The Hamiltonian which we used is as follows:

$$\mathcal{H} = \mathcal{H}_{\text{CEF}} + \mathcal{H}_Q + \mathcal{H}_8 + \mathcal{H}_b + \mathcal{H}_{\text{ex}} + \mathcal{H}_{\text{Zeeman}}, \quad (\text{A1})$$

$$\begin{aligned} \mathcal{H}_Q = & - \sum_{ij} K_5 [O_{xy}(i)O_{xy}(j) \\ & + O_{yz}(i)O_{yz}(j) + O_{zx}(i)O_{zx}(j)], \end{aligned} \quad (\text{A2})$$

$$\mathcal{H}_{xyz} = - \sum_{ij} K_8 T_{xyz}(i)T_{xyz}(j), \quad (\text{A3})$$

$$\mathcal{H}_\beta = - \sum_{ij} K_b T_\beta(i)T_\beta(j), \quad (\text{A4})$$

$$\mathcal{H}_{\text{ex}} = - \sum_{ij} J_{\text{ex}} \mathbf{J}(i) \cdot \mathbf{J}(j), \quad (\text{A5})$$

$$\mathcal{H}_{\text{Zeeman}} = \sum_i g_J \mu_B \mathbf{H} \cdot \mathbf{J}(i). \quad (\text{A6})$$

Here, $O_{xy} = \frac{\sqrt{3}}{2}(J_x J_y + J_y J_x)$, etc., $T_{xyz} = \frac{\sqrt{15}}{6} J_x J_y J_z = \frac{\sqrt{15}}{6}(J_x O_{yz} + J_y O_{zx} + J_z O_{xy})$, $T_\beta = (T_\beta^x + T_\beta^y + T_\beta^z)/3$, $T_\beta^x = \frac{\sqrt{15}}{6}(J_x J_y^2 - J_y^2 J_x)$, etc., and $J_x J_y^2 = (J_x J_y^2 + J_y J_x J_y + J_y^2 J_x)/3$, etc. In the four-sublattice model, the Hamiltonian is expressed as follows:

$$\mathcal{H} = \mathcal{H}^{\text{AA}} + \mathcal{H}^{\text{AB}} + \mathcal{H}^{\text{BA}} + \mathcal{H}^{\text{BA}}, \quad (\text{A7})$$

$$\mathcal{H}^{\text{AA}} = \sum_{i \in \text{AA}} h_i^{\text{AA}}, \text{ etc.}, \quad (\text{A8})$$

$$h_i^{\text{AA}} = h_{Q,i}^{\text{AA}} + h_{\text{oct},i}^{\text{AA}} + h_{\text{ex},i}^{\text{AA}} + h_{\text{Zeeman},i}^{\text{AA}}, \quad (\text{A9})$$

$$\begin{aligned} h_{Q,i}^{\text{AA}} = & -K_5 [(\langle O_{xy} \rangle_{av}^{\text{BA}} + \langle O_{xy} \rangle_{av}^{\text{BB}}) O_{xy}(i) \\ & + (\langle O_{yz} \rangle_{av}^{\text{BA}} + \langle O_{yz} \rangle_{av}^{\text{BB}}) O_{yz}(i) \\ & + (\langle O_{zx} \rangle_{av}^{\text{BA}} + \langle O_{zx} \rangle_{av}^{\text{BB}}) O_{zx}(i)] \end{aligned} \quad (\text{A10})$$

$$h_{8,i}^{\text{AA}} = K_8 \langle T_{xyz} \rangle_{av}^{\text{BA}} T_{xyz}(i), \quad (\text{A11})$$

$$h_{b,i}^{\text{AA}} = K_b \langle T_\beta \rangle_{av}^{\text{BA}} T_\beta(i), \quad (\text{A12})$$

$$\begin{aligned} h_{\text{ex},i}^{\text{AA}} = & J_{\text{ex}}^{\text{intraQ}} [\langle J_x \rangle_{av}^{\text{AB}} J_x(i) + \langle J_y \rangle_{av}^{\text{AB}} J_y(i) + \langle J_z \rangle_{av}^{\text{AB}} J_z(i)] \\ & - J_{\text{ex}}^{\text{interQ}} [(\langle J_x \rangle_{av}^{\text{BA}} + \langle J_y \rangle_{av}^{\text{BB}}) J_y(i) \\ & + (\langle J_z \rangle_{av}^{\text{BA}} + \langle J_z \rangle_{av}^{\text{BB}}) J_z(i)]. \end{aligned} \quad (\text{A13})$$

$\langle O_{xy} \rangle_{av}^{\text{BA}}$ means the thermal average of O_{xy} of the BA sublattice, etc.; h_i^{AB} , h_i^{BA} , h_i^{BB} are similar to h_i^{AA} apart from the sites producing the mean field. For example, the difference between h_i^{AB} and h_i^{BA} is the intra- Q AF exchange interaction, i.e., $-J_{\text{ex}}^{\text{intraQ}} [(\langle J_x \rangle_{av}^{\text{AA}} J_x(i) + \langle J_y \rangle_{av}^{\text{AA}} J_y(i) + \langle J_z \rangle_{av}^{\text{AA}} J_z(i))]$ for h_i^{AB} . The magnetic field is applied along the z axis.

In this paper, tentatively we call the AFQ and AFM phases obtained by the calculation phase II and III, respectively. We also call tentatively the critical field from the AFM to AFQ phase and that from the paramagnetic to AFQ phase obtained by the calculation $H_c^{\text{III-II}}$ and $H_c^{\text{I-II}}$, respectively.

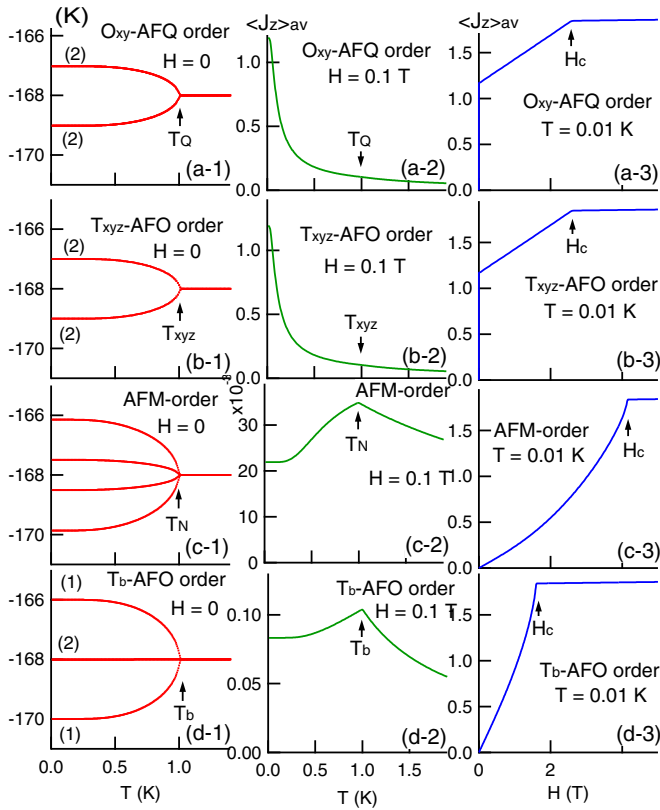


FIG. 8. (a-1)–(d-1) Temperature dependence of the quartet energy levels, (a-2)–(d-2) temperature dependence of $\langle J_z \rangle_{av}$ at $H = 0.1$ T, (1-3)–(d-3) magnetic field dependence of $\langle J_z \rangle_{av}$ at $T = 0$ K for O_{xy} -AFQ, T_{xyz} -AFO, AFM, and T_β -AFO order with the transition temperature of 1 K, respectively. The number inside the brackets in (a-1), (b-1), and (d-1) indicates the spin degeneracies.

1. LRO by the four different interactions

Here, we show the T dependence of the energy levels at $H = 0$ and $\langle J_z \rangle_{av}$ at $H = 0.1$ T along the z direction at $T = 0$ K for the four types of LRO, where each interaction exists independently. Here, the transition temperature is assumed to be 1 K in all cases. T_Q , T_{xyz} , T_N , and T_b is defined as the transition temperature for the O_{xy} -AFQ, T_{xyz} -AFO, AFM, and T_β -AFO interaction, respectively. We define T_Q^0 as the bare T_Q , which is the transition temperature for the case in which the O_{xy} -AFQ interaction exists independently, etc. Hereafter, we use T_Q^0 as the magnitude of the O_{xy} -AFQ interaction, etc.

Figures 8(a-1)–8(a-3) show the T dependencies of the quartet energy levels at $H = 0$ and $\langle J_z \rangle_{av}$ at $H = 0.1$ T and the $\langle J_z \rangle_{av}$ - H curve at $T = 0.01$ K in the case of O_{xy} -AFQ order with the transition temperature of 1 K. Figures 8(b-1)–8(b-3), 8(c-1)–8(c-3), and 8(d-1)–8(d-3) show those for the T_{xyz} -AFO, AFM, and T_β -AFO order, respectively.

In the O_{xy} -AFQ order, the quartet is split into the two doublets below T_Q with the total energy-level splitting of 2 K at $T = 0$ K. $\langle J_z \rangle_{av}$ at $H = 0.1$ T exhibits a small anomaly at T_Q^0 and a Curie-like temperature dependence below T_Q^0 due to the twofold spin degeneracies in the doublet ground state as shown in Fig. 8(a-2). $\langle J_z \rangle_{av}$ at $T = 0$ K shows a finite magnitude of 7/6 at the infinitesimally small magnetic field because of

the twofold spin degeneracy in the doublet at $H = 0$. $\langle J_z \rangle_{av}$ exhibits an H -linear increase up to 11/6 at the saturation field, $H_c = 2.6$ T.

In the T_{xyz} -AFO order, the Γ_8 quartet is split into the two doublets below T_{xyz}^0 , where the magnitude of the energy-level splitting at $T = 0$ K is 2 K. The total-energy level splitting is 2 K as in the case of the O_{xy} -AFQ order. The T and H dependencies of $\langle J_z \rangle_{av}$ are the same as those in the O_{xy} -AFQ order.

In the AFM order shown in Figs. 8(c-1)–8(c-3), the quartet is split into the four levels below T_N^0 . The total-energy-level splitting is ~ 3.8 K, which is about twice larger than 2 K in the above two cases. The spins below T_N^0 are oriented to the fourfold axis, which originates from the cubic CEF potential. The T dependence of $\langle J_z \rangle_{av}$ exhibits a finite magnitude at $T = 0$ K and a peak at T_N . This is because $\langle J_z \rangle_{av}$ exhibits a spin canted magnetization process showing a concave H dependence up to $H_c = 4.2$ T, which is roughly twice larger than 2.6 T in the above two cases.

In the T_β -AFO order shown in Figs. 8(d-1)–8(d-3), the quartet is split into the three levels (singlet-doublet-singlet) below T_b^0 . The total-energy splitting is 4 K, which is twice larger than 2 K in Figs. 8(a-1) and 8(b-1). $\langle J_z \rangle_{av}$ exhibits a finite magnitude at $T = 0$ K, which originates from the van Vleck contribution from the excited doublets. At T_b^0 , $\langle J_z \rangle_{av}$ exhibits a peak. $\langle J_z \rangle_{av}$ exhibits a concave H dependence up to $H_c = 1.6$ T.

2. LRO when the two different interactions with the different magnitudes coexist

Here, we show the results of the case in which the two different types of the interaction coexist. We assume that the higher bare transition temperature is 1 K and the lower one is 0.7 K. Figures 9(a-1)–9(g) show the T dependence of the quartet energy levels at $H = 0$ and 0.1 T. $\langle J_z \rangle_{av}$ at $H = 0.1$ T and the $\langle J_z \rangle_{av}$ - H curve at $T = 0.01$ K for the six different types of the coexistence of the two different interactions.

Figures 9(a-1)–9(a-3) shows the results under the condition of $T_Q^0 = 1$ K and $T_{xyz}^0 = 0.7$ K. The quartet is split into the two doublets below T_Q^0 and these doublets are split into the four levels below T_{xyz} . T_{xyz} is reduced to 0.55 K from $T_{xyz}^0 = 0.7$ K. At $H = 0$, the spontaneous magnetization appears below T_Q and $\langle J_z \rangle_{av}$ is 7/6 at $T = 0.01$ K. However, when $H = 0.1$ T, T_{xyz} disappears and $\langle J_z \rangle_{av}$ shows only one anomaly at T_Q . Namely, the transition at T_{xyz} appears only at $H = 0$. As for the H dependence, $\langle J_z \rangle_{av}$ exhibits a finite magnitude of 7/6 at the infinitesimally small magnetic field and shows an H -linear increase up to 11/6 at $H_c = 4.5$ T. When $T_{xyz}^0 = 1$ K and $T_Q^0 = 0.7$ K, the same results are obtained.

Figures 9(b-1)–9(b-3) show the results for $T_Q^0 = 1$ K and $T_N^0 = 0.7$ K. The quartet is split into the two doublets below T_Q^0 and these are split into the four levels below T_N . T_N = 0.64 K is reduced from $T_N^0 = 0.7$ K. Although $\langle J_z \rangle_{av}$ exhibits a clear anomaly at T_N , an anomaly at T_Q is quite small. $\langle J_z \rangle_{av}$ exhibits an H -linear increase in the AFM phase up to 2.5 T and above this field, M exhibits again an H -linear increase up to 11/6 at $H_c = 5.0$ T.

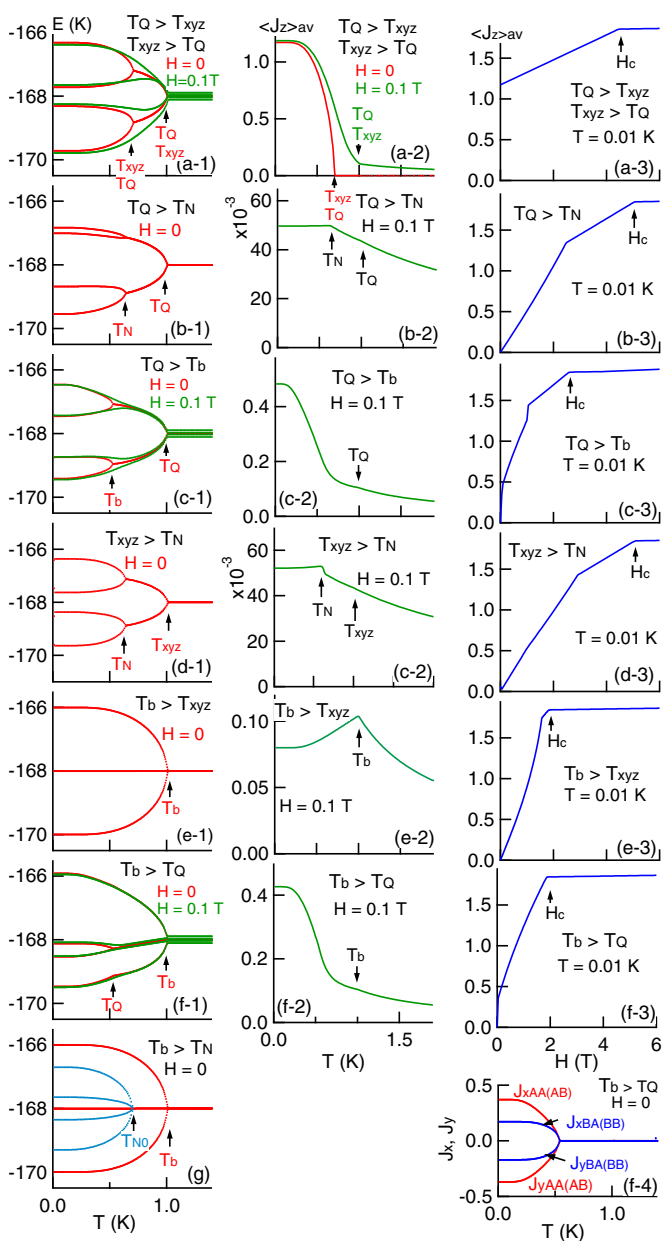


FIG. 9. (a-1)–(e-1) Temperature dependence of the quartet energy levels. (a-2)–(e-2) Temperature dependencies of $\langle J_z \rangle_{av}$ at $H = 0.1$ T. (a-3)–(e-3) H dependence of $\langle J_z \rangle_{av}$ at $T = 0.01$ K for (a-1)–(a-3) T_{xyz}^0 (or T_Q^0) = 0.7 K and T_Q^0 (T_{xyz}^0) = 1 K. (b-1)–(b-3) $T_Q^0 = 1$ K and $T_N^0 = 0.7$ K. (c-1)–(c-3) $T_Q^0 = 1$ K and $T_b^0 = 0.7$ K. (d-1)–(d-3) $T_{xyz}^0 = 1$ K and $T_N^0 = 0.7$ K. (e-1)–(e-3) $T_b^0 = 1$ K and $T_{xyz}^0 = 0.7$ K. (f-1)–(f-4) $T_b^0 = 1$ K and $T_Q^0 = 0.7$ K, respectively. (f-4) AFM components below T_Q . (g) Temperature dependence of the quartet energy levels $T_b^0 = 1$ K and $T_N^0 = 0.7$ K. In this case there are always only T_β -AFQ orders. See the text for details.

Figures 9(c-1)–9(c-3) show the results for $T_Q^0 = 1$ K and $T_b^0 = 0.7$ K. This corresponds to the II \rightarrow IV phase transition and the corresponding experimental results are shown in Figs. 5(c) and 5(d). The quartet is split into the two doublets below T_Q^0 and these are split into the four levels below $T_b = 0.64$ K, which is reduced from $T_N^0 = 0.7$ K. The transition at T_b^0 appears only at $H = 0$. Below T_b , the AFM components along

the twofold axis appear in the xy plane, although the AFM interaction is not taken into account in the present case. The appearance of the AFM components are obtained also below T_Q under the condition of $T_b^0 = 1$ K and $T_Q^0 = 0.7$ K. $\langle J_z \rangle_{av}$ at $H = 0.1$ T exhibits a kink at $T_Q = 1$ K and increases with decreasing temperature. Different from the result of Fig. 9(a-2), a spontaneous magnetization at $H = 0$ does not appear below T_b .

Figures 9(d-1)–9(d-3) show the results under the condition of $T_{xyz}^0 = 1$ K and $T_N^0 = 0.7$ K. The quartet is split into the two doublets below T_{xyz}^0 and these are split into the four levels below $T_N = 0.64$ K, which is reduced from $T_N^0 = 0.7$ K. Although $\langle J_z \rangle_{av}$ exhibits a clear kink at $T_N = 0.64$ K, the anomaly at T_{xyz} is quite small. The $\langle J_z \rangle_{av}$ - H curve shows the two anomalies at $H = 2.9$ and 5.0 T. The spin canted process is realized up to 2.9 T and above this field the T_{xyz} -AFQ ordered state is realized.

Figures 9(e-1)–9(e-3) show the results under the condition of $T_b^0 = 1$ K and $T_{xyz}^0 = 0.7$ K. The quartet is split into the three levels of the singlet-doublet-singlet below $T_b^0 = 1$ K. The results are nearly the same as those in the single T_β -AFQ order in Fig. 8(d-1). The T_{xyz} -AFQ order does not appear. A small difference is the magnitude of $\langle J_z \rangle_{av}$ at $T = 0$ K. It is 0.0799 in the present case, while it is 0.0833 in the T_β -AFQ order in Fig. 8(d-1). Thus, the T_{xyz} -AFQ interaction affects little the T_β -AFQ order. $\langle J_z \rangle_{av}$ exhibits a concave H dependence up to 1.6 T as in Fig. 9(e-3). Above 1.6 T up to 1.8 T, the T_{xyz} -AFQ order appears. $H_c = 1.8$ T is much smaller than those of the above three cases.

Figures 9(f-1)–9(f-3) show the results under the condition of $T_b^0 = 1$ K and $T_Q^0 = 0.7$ K. The quartet is split into the three levels (singlet-doublet-singlet) below T_b^0 and the two singlets exhibit a kink and the doublet is split into the two levels below $T_Q = 0.52$ K. The T dependence of the energy levels below T_b is asymmetric, different from the symmetric one in Fig. 9(e-1). This originates from the suppression of $O_{xy} + O_{yz} + O_{zx}$ -FQ order by the O_{xy} -type AFQ interaction. At $H = 0.1$ T, T_Q disappears as in the case of Fig. 9(a-2). $\langle J_z \rangle_{av}$ at $H = 0.1$ T exhibits a small kink at $T_b^0 = 1$ K and $\langle J_z \rangle_{av}$ increases with decreasing temperature, different from a sharp peak at T_b in Fig. 9(e-2). Figure 9(f-4) shows the T dependence of the AFM component below T_Q . The AFM component is along the twofold axis in the xy plane. This AFM component is not induced by the AFM interaction but by the AFQ order without the spin degeneracy. It is known that when the magnetic field is applied to the O_2 -AFQ ordered state, the AFM component with the magnitude of $(\frac{11}{6} - \frac{1}{2})$ is induced along the z axis. In the present case, the similar type of AFQ order is produced in the O_{xy} -AFQ order below T_Q in the $O_{xy} + O_{yz} + O_{zx}$ -FQ order below T_b . There, the spins are induced in each sublattice below T_Q . The induced spins are along the twofold axis and its magnitude is different between the (AA, AB) and (BA, BB) sublattices. This difference induces the AFM component along the twofold axis.

Figure 9(g) shows the T dependence of the quartet at $H = 0$ under the condition of $T_b^0 = 1$ K and $T_N^0 = 0.7$ K. This figure does not mean that the AFM order appears below T_b^0 and only one transition exists at $T_b^0 = 1$ K. As far as $T_N^0 < T_b^0$, the AFM order does not appear. As is seen in Figs. 8(c-1) and 8(d-2),

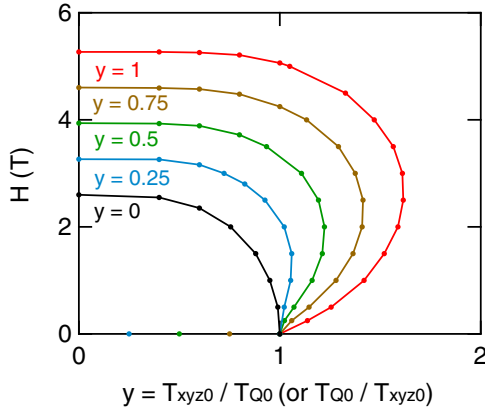


FIG. 10. Magnetic phase diagrams when the O_{xy} -AFQ and T_{xyz} -AFO interaction coexist. y is the ratio of these two interactions, i.e., $y = T_{xyz}^0/T_Q^0$ or T_Q^0/T_{xyz}^0 , where the interaction of the denominator is 1 K. See the text for details.

the lowest energy of -169.8 K at $T = 0$ K for $T_N^0 = 1$ K is higher than -170 K for $T_b^0 = 1$ K. This means that even when $T_N^0 = T_b^0$, the AFM order does not appear. Here, we note that when the O_{xy} -AFQ interaction is introduced, the AFM order could appear.

3. Magnetic phase diagram when O_{xy} -type AFQ and the T_{xyz} -AFO orders coexist

Here, we show how the magnetic phase diagram is varied when the ratio of the O_{xy} -AFQ or T_{xyz} -AFO interactions is changed. We use, as its ratio, $y = T_{xyz}^0/T_Q^0$ or T_Q^0/T_{xyz}^0 and $T_Q^0 = 1$ K in the former and $T_{xyz}^0 = 1$ K in the latter.

Figure 10 shows the magnetic phase diagrams for $y = 0, 0.25, 0.5,$ and 1 . We note that the same results are obtained in both cases of $T_Q^0 > T_{xyz}^0$ and $T_{xyz}^0 > T_Q^0$. Although at $H = 0$, the two phase transitions exist, only one transition temperature exists in finite magnetic fields. When the O_{xy} -AFQ and T_{xyz} -AFO interactions coexist, the enhancement of the transition temperature with increasing magnetic field appears. Its enhancement is largest for $y = 1$ and is reduced with decreasing y . The enhancement of T_Q is observed in $\text{Ce}_x\text{La}_{1-x}\text{B}_6$ regardless of the x values. The present results indicate that the O_{xy} -AFQ order is realized for $x > 0.82$ and the T_{xyz} -AFO order for $x < 0.8$.

4. Case when the two or three interactions coexist

In the previous section, we showed the results under the condition of $T_Q^0 = 1$ K and $T_N^0 = 0.7$ K, etc., in Fig. 9. Here, we show how T_N is varied by changing T_N^0 under $T_Q^0 = 1$ K, etc., at $H = 0$.

We take the higher bare transition temperature as 1 K. The lower bare transition temperature is varied between 0 and 1 K. Figure 11(a) shows the T_N^0 or T_{xyz}^0 dependence of T_{xyz} and T_N under the condition of $T_Q^0 = 1$ K. T_{xyz} is proportional to T_{xyz}^0 . T_N is smaller than T_N^0 for $x < 0.8$ and higher than T_N^0 for $x > 0.8$. Figure 11(b) shows the T_Q^0 or T_N^0 dependence of T_Q or T_N under the condition of $T_{xyz}^0 = 1$ K. T_Q is proportional to T_Q^0 . T_N is slightly smaller than T_N^0 for $0 \text{ K} < T_N^0 < 1 \text{ K}$.

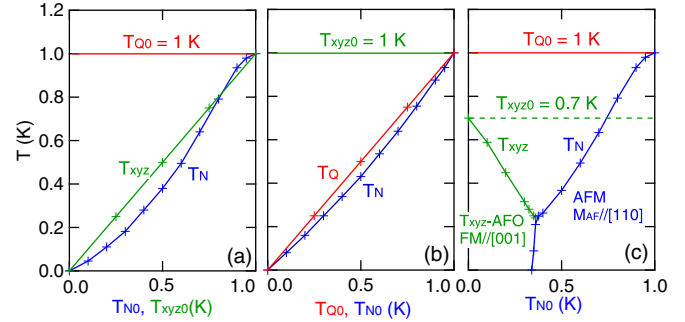


FIG. 11. (a) T_N^0 or T_{xyz}^0 dependence of the real transition temperature, T_N or T_{xyz} , when the AFM or T_{xyz} -AFO orders coexist with the O_{xy} -AFQ order under the condition of $T_Q^0 = 1$ K. (b) T_Q^0 or T_N^0 dependence of T_N or T_{xyz} under the condition of $T_{xyz}^0 = 1$ K. (c) T_N^0 dependence of T_{xyz} or T_N under the condition of $T_Q^0 = 1$ K and $T_{xyz}^0 = 0.7$ K at $H = 0$. See the text for details.

Figure 11(c) shows the T_N^0 dependence of T_{xyz} or T_N under the condition of $T_Q^0 = 1$ K and $T_{xyz}^0 = 0.7$ K. When $T_N^0 = 0$ K, the T_{xyz} -AFO order appears at $T_{xyz} = 0.7$ K, below which the spontaneous magnetization appears along the z direction. With increasing T_N^0 , the AFM interaction acts to suppress both T_{xyz} and the magnitude of the spontaneous magnetization. Above $T_N^0 = 0.35$ K, the T_{xyz} -AFO order disappears and in place, the AFM order appears and T_N increases with increasing T_N^0 . In the AFM ordered state, the spins are noncollinear and oriented to the twofold axis in the xy plane.

5. T_N^0 or T_Q^0 dependence of T_N or T_Q for $T_b^0 = 1$ K

Here, we investigate the condition for the appearance of the AFM order under the condition of $T_b^0 = 1$ K. As was shown in the previous section, the AFM order does not appear as far as $T_b^0 > T_N^0$. In this subsection, we show that the AFM order could appear when the O_{xy} -AFQ order coexists.

First, we show the $T_Q^0, T_{xyz}^0,$ or T_N^0 dependence of $T_Q, T_{xyz},$ or T_N under the condition of $T_b^0 = 1$ K at $H = 0$, which is shown in Fig. 12. T_{xyz} and T_N are always zero as was shown in Figs. 9(e-1) and 9(g). T_Q does not exist up to $T_Q^0 = 0.5$ K and suddenly increases up to ~ 0.3 K at $T_Q^0 \sim 0.5$ K and increases roughly linear to T_Q^0 above ~ 0.5 K. Below T_Q , the intermediate doublet is split into the two levels as is shown in Fig. 9(e-1).

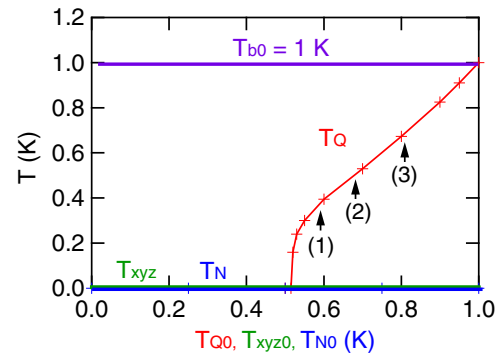


FIG. 12. $T_Q^0, T_{xyz}^0,$ or T_N^0 dependence of the real transition temperature, $T_{xyz}, T_N,$ and T_Q under the $T_b^0 = 1$ K at $H = 0$. See the text for details.

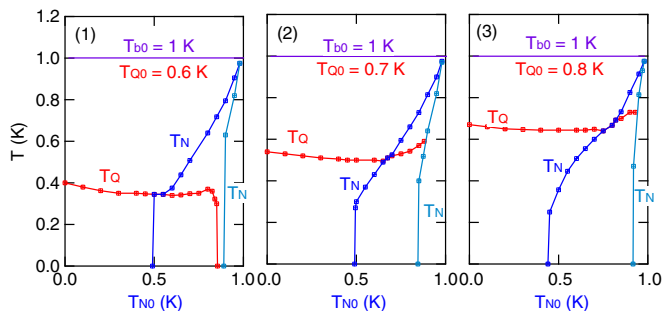


FIG. 13. T_N^0 dependence of the real transition temperature, T_Q and T_N , when the AFM, T_β -AFO, and O_{xy} -AFQ orders coexist with the T_β -AFO order under the condition of $T_b^0 = 1$ K and (1) $T_Q^0 = 0.6$ K, (2) $T_Q^0 = 0.7$ K, and (3) $T_Q^0 = 0.8$ K. See the text for details.

Next, we show how the AFM order appears in the three cases of (1)–(3) indicated by the arrows in Fig. 12. The T_N^0 dependence of T_Q and T_N under $T_b^0 = 1$ K and $T_Q^0 = 0.6$ K, which is shown in Fig. 13(1) corresponds to case (1) in Fig. 12(d). T_Q at $T_N^0 = 0$ K is 0.4 K, which is reduced from $T_Q^0 = 0.6$ K and decreases slightly with increasing T_N^0 . There exists only one transition at T_Q below $T_N^0 = 0.48$ K. At $T_N^0 = 0.48$ K, the AFM order with $T_N = 0.36$ K suddenly appears, where the AFM components appear along the z axis. Namely, the AFM order with the three components of spin, J_x , J_y , and J_z are realized. There, $T_N = 0.36$ K and coincides with $T_Q = 0.36$ K. The sudden appearance of T_N is due to the nonmagnetic-magnetic transition. The magnitude of the AFM components increases with increasing T_N^0 . $T_Q = T_N$ is fulfilled in a small T_N^0 region up to 0.55 K, above which T_Q and T_N separate. T_Q is roughly constant and T_N increases with increasing T_N^0 . T_Q suddenly disappears at $T_N^0 = 0.84$ K and in its place another type of T_N appears above $T_N^0 = 0.9$ K, where the spins are oriented to the fourfold axis and T_β -AFO order disappears.

The T_N^0 dependence of T_Q and T_N under the condition of $T_b^0 = 1$ K and $T_Q^0 = 0.7$ K shown in Fig. 13(2) corresponds to case (2) in Fig. 12, although there exists only one transition

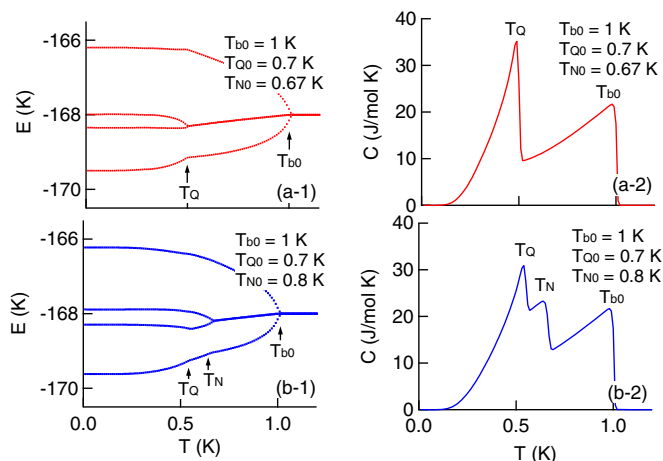


FIG. 14. (a-1), (b-1) Temperature dependencies of the quartet energy levels. (a-2), (b-2) Temperature dependencies of the specific heat for $(T_b^0, T_Q^0, T_N^0) = (1 \text{ K}, 0.7 \text{ K}, 0.67 \text{ K})$ and $(1 \text{ K}, 0.7 \text{ K}, 0.8 \text{ K})$, respectively.

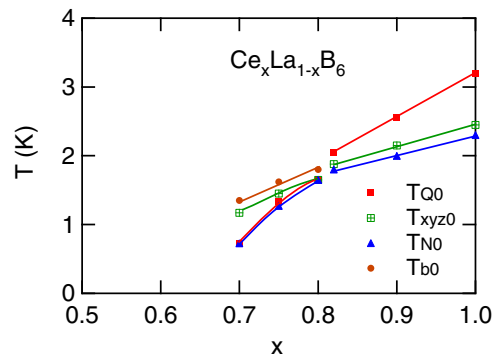


FIG. 15. x dependencies of the bare O_{xy} -AFQ, T_{xyz} -AFO, AFM, and T_β -AFO interaction used in the calculation for the four sublattice model to obtain the magnetic phase diagrams of $\text{Ce}_x\text{La}_{1-x}\text{B}_6$.

at T_Q up to $T_N^0 = 0.48$ K, above which the AFM order with $T_N = 0.34$ K appears. T_N increases with increasing T_N^0 and T_N coincides with T_Q between 0.63 and 0.68 K, above which T_Q and T_N separate again. The increase of T_N with increasing T_N^0 is rather rapid but that of T_Q is small. Above $T_N^0 = 0.83$ K, the AFM order with spins along the fourfold axis appears and the T_β -AFO order disappears.

The T_N^0 dependence of T_Q and T_N for $T_b^0 = 1$ K and $T_Q^0 = 0.8$ K shown in Fig. 13(3) corresponds to case (3) in Fig. 12. The T_N^0 dependence is similar to that in case (2), while the region of $T_Q = T_N$ is shifted to $T_N^0 \sim 0.8$ K.

Figures 14(a-1) and 14(a-2) show the T dependence of the quartet energy levels and specific heat for $T_b^0 = 1$ K and $T_Q^0 =$

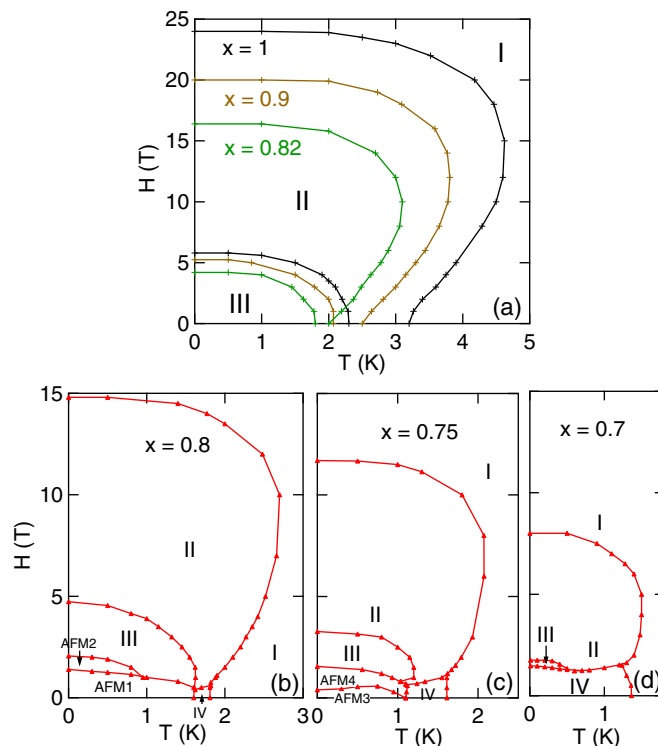


FIG. 16. Calculated magnetic phase diagrams of $\text{Ce}_x\text{La}_{1-x}\text{B}_6$; (a) $x = 1 \sim 0.82$, (b) $x = 0.8$, (c) $x = 0.75$, and (d) $x = 0.7$.

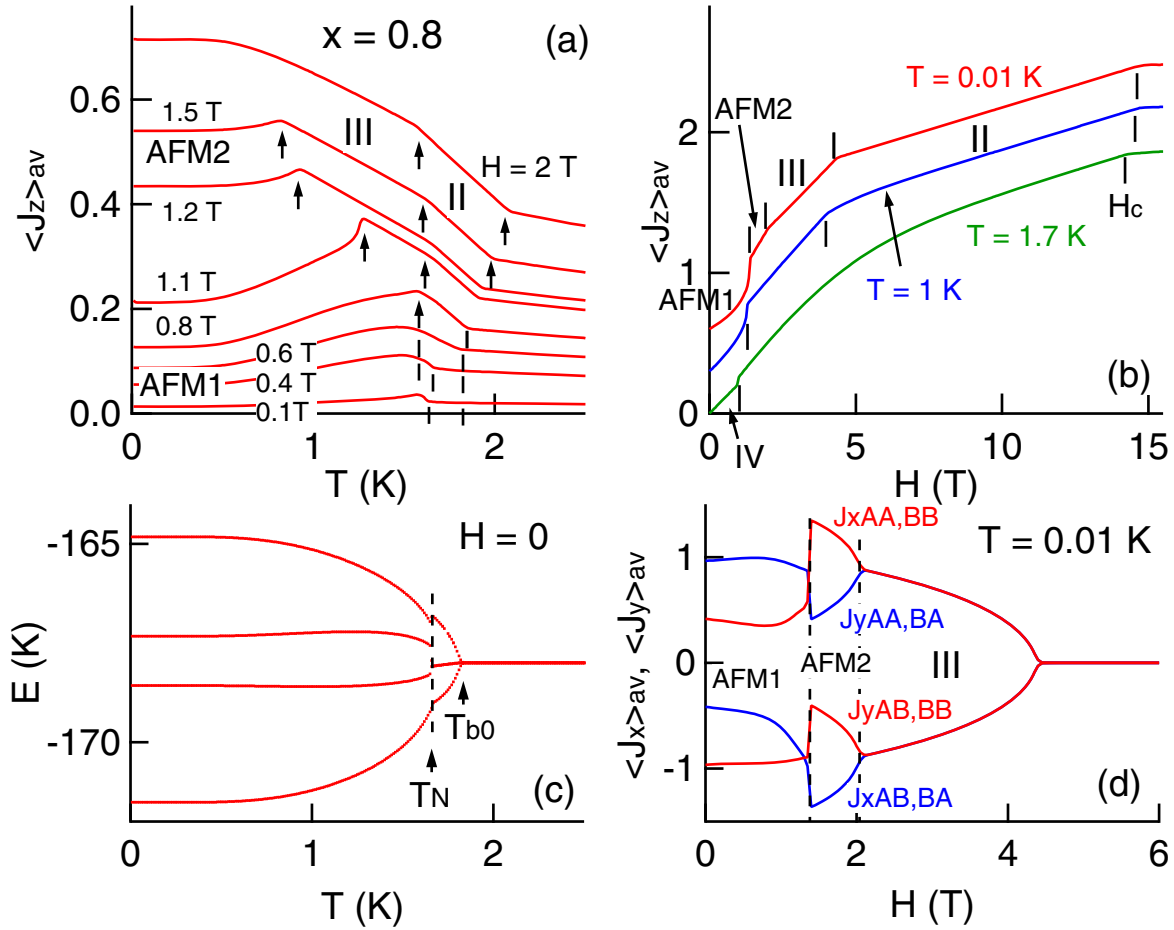


FIG. 17. Temperature dependence of $\langle J_z \rangle_{av}$ in magnetic fields. (b) Magnetic field dependencies of $\langle J_z \rangle_{av}$. (c) Temperature dependence of the quartet energy levels at $H = 0$. (d) Magnetic field dependence of the antiferrocomponent $\langle J_z \rangle_{av}$, $\langle J_y \rangle_{av}$ in the xy plane for $x = 0.8$. In (b), the origin of the vertical axis is shifted in each curve.

0.7 K and $T_N^0 = 0.67$ K, respectively. Figures 14(b-1) and 14(b-2) show those for $T_b^0 = 1$ K, $T_Q^0 = 0.7$ K, and $T_N^0 = 0.8$ K. In the former, only one transition appears at $T_Q = 0.5$ K, below which the AFM ordered state accompanied with the O_{xy} -AFQ order is realized. In the latter, the two transitions appear at $T_Q = 0.52$ K and $T_N = 0.7$ K in the T_β -AFO ordered state.

6. Magnetic phase diagrams of $\text{Ce}_x\text{La}_{1-x}\text{B}_6$ obtained by calculation

To reproduce the magnetic phase diagram of $\text{Ce}_x\text{La}_{1-x}\text{B}_6$, it is necessary to determine the magnitude of the four interactions of O_{xy} -AFQ, T_{xyz} -AFO, AFM, T_β -AFO. We used the x dependencies of the four interactions as shown in Fig. 15, according to the following consideration. Since for $x > 0.82$, T_Q and T_N are known from the experiments, T_Q^0 and T_N^0 are determined to reproduce the experimental results. As for T_{xyz}^0 , it is determined to reproduce the magnetic phase diagram which shows a characteristic enhancement of T_Q in the magnetic field. For $x < 0.8$, T_{IV} is known from the experiments, T_b^0 is determined to reproduce T_{IV} . While there is no information on T_{xyz} -AFO interaction for $x < 0.8$, we assumed the x dependence of T_{xyz}^0

in Fig. 15 according to the following reasons. A considerable magnitude of the T_{xyz} -AFO interaction should exist also for $x < 0.8$, considering that the enhancement of the II-I phase boundary in magnetic fields is still pronounced. Furthermore, as was discussed in the previous section, T_{xyz}^0 does not affect the T_β -AFO order as far as $T_{xyz}^0 < T_b^0$. Thereby, we assumed that T_{xyz}^0 is slightly smaller than T_b^0 for $x < 0.8$ as shown in Fig. 17. As for T_Q^0 and T_N^0 , based on the results in Fig. 15, so as to reproduce the experimentally observed T_N , we assume their x dependencies as shown in Fig. 15.

The calculated magnetic phase diagrams of $\text{Ce}_x\text{La}_{1-x}\text{B}_6$ are shown in Figs. 16(a)–16(d) for $x > 0.82$, $x = 0.8$, 0.75, and 0.7, respectively. The obtained results are similar, $x > 0.82$, rather consistent with the experimental results. Also for $x < 0.8$, the characteristics of the magnetic phase diagram could be reproduced qualitatively. For $x = 0.8$ and 0.75, phases II, III, and IV could be reproduced, although the AFM order at low fields is different from that of phase III. For $x = 0.7$, the ground state at low fields is the T_β -AFO ordered state (phase IV) and phase III appears at the finite magnetic field inside phase II, as observed in the experiments. Here, we note that although the enhancement of the I-II transition

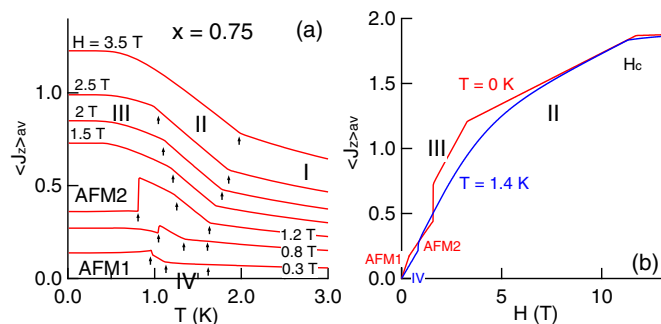


FIG. 18. (a) Temperature dependence of $\langle J_z \rangle_{av}$ in magnetic fields and (b) magnetic field dependence of $\langle J_z \rangle_{av}$ for $x = 0.75$.

temperature in magnetic fields is pronounced for $x > 0.8$, it is rapidly suppressed with decreasing x below 0.75. For $x = 0.7$, it is quite small. This is because when the ratio of T_{xyz}^0 and T_Q^0 is close to 1, the enhancement is large, but when the ratio is small, it is small. For $x < 0.75$, since the ratio of T_Q^0/T_{xyz}^0 is rapidly reduced, the enhancement of the I-II phase boundary is reduced rapidly with decreasing x . Furthermore, the enhancement is expected to disappear for $x < 0.65$ because T_Q^0 disappears. These clearly contradict the experimental results.

Figures 17(a)–17(d) show the T and H dependencies of $\langle J_z \rangle_{av}$ for $x = 0.8$, the T dependence of the quartet energy levels, and H dependence of the antiferrocomponents, J_x and J_y , respectively. Here, $(T_N^0, T_Q^0, T_{xyz}^0, T_b^0) = (1.65$ K, 1.65 K, 1.65 K, 1.8 K) are used in the calculation. At $H = 0$, the quartet is split into the three levels below $T_b^0 = 1.8$ K and these are split into the four levels below $T_N = 1.65$ K. The characteristic properties in phases II and III could be reproduced rather well. However, at low magnetic fields, the AFM order different from that of the phase III appears. In the AFM1 phase, the AFM order with the antiparallel component along the z axis is realized, which leads to the concave H dependence of the $\langle J_z \rangle_{av}$ - H curve. In the AFM2 phase, the AFM component along the z axis disappears and the AFM components exist only in the xy plane, which is shown in Fig. 17(d). This leads to the spin canting magnetization process in this phase. Above 1 K, the AFM2 phase disappears and the direct AFM1-III transition takes place. In phase III, the AFM components are located in the xy plane along the twofold axis, which is shown in Fig. 19(d).

Figures 18(a) and 18(b) show the T and H dependencies of $\langle J_z \rangle_{av}$ for $x = 0.75$, respectively. Here, $(T_N^0, T_Q^0, T_{xyz}^0, T_b^0) = (1.27$ K, 1.25 K, 1.45 K, 1.62 K) are used in the calculation. $T_b = 1.62$ K and $T_N = 1.1$ K are obtained at $H = 0$. Phase III and II are obtained above 1.6 and 3.4 T, respectively. At low magnetic field, the AFM3 phase is obtained below 0.4 T and

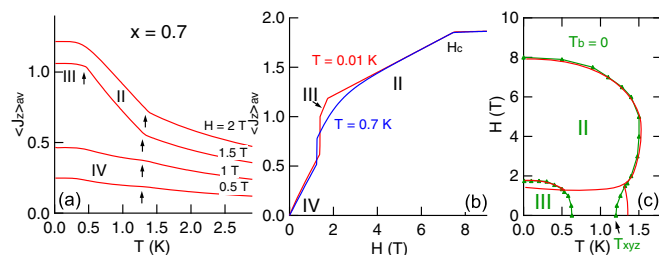


FIG. 19. (a) Temperature dependence of $\langle J_z \rangle_{av}$ in magnetic fields, (b) magnetic field dependencies of $\langle J_z \rangle_{av}$ and (c) magnetic phase diagram for $x = 0.7$. In (c), the magnetic phase diagram indicated by the green symbols is that without the T_β -AFO order. The red one is the same one as shown in Fig. 18(d).

the AFM4 one up to 1.6 T. In the AFM3 phase, the spins are along the fourfold axis in the xy plane and in the AFM4 phase, the antiferrocomponents along the z axis exist. The AFM order at low fields for $x < 0.8$ could not be uniquely determined but could be different, depending on the subtle difference of the four interactions.

Figures 19(a) and 19(b) show the magnetization curve and the T dependence of $\langle J_z \rangle_{av}$ for $x = 0.7$, respectively. Here, $(T_N^0, T_Q^0, T_{xyz}^0, T_b^0) = (0.73$ K, 0.73 K, 1.18 K, 1.35 K) are used in the calculation. The ground state at low fields is always phase IV below $T_b = 1.35$ K without showing another transition down to $T = 0$ K. However, phase III appears below $T_N = 0.55$ K in a finite field region between 1.5 and 1.75 T. $\langle J_z \rangle_{av}$ does not show a peak at T_{IV} in the same way as for $x = 0.75$. Figure 19(c) shows a magnetic phase diagram for $x = 0.7$. The red line is the same as that in Fig. 18 and the green one is obtained by the calculation without T_β -AFO interaction. Above 1.5 T, the magnetic phase diagram is the same as that in Fig. 16(a). However, it is different below this field. Phase II appears at 1.2 K and phase III at 0.65 K, which is similar to that of CeB₆. Since T_Q^0 is much smaller than T_{xyz}^0 for $x = 0.7$, the transition is not by the O_{xy} -AFQ order but by the T_{xyz} -AFO order as indicated in Fig. 10.

In the present calculation, the following problems are found to appear. For example, in Ce_{0.7}La_{0.3}B₆, although T_N in magnetic field is roughly the same as T_{IV} at $H = 0$ as shown in Fig. 9(c), the calculated T_N is much less than T_b^0 . A peak of the magnetic susceptibility at T_{IV} could not be reproduced in the present calculation, which originates from the competition between the $O_{xy} + O_{yz} + O_{zx}$ -FQ order in phase IV and the O_{xy} -AFQ interaction as pointed out by Kondo and Sera. For $x = 0.6$, T_Q^0 and T_N^0 are expected to disappear, although the experimental results show that as far as phase II exists in magnetic fields, the enhancement of the I-II transition temperature is pronouncedly enhanced with increasing magnetic field.

- [1] P. Santini, S. Carretta, G. Amoretti, R. Caciuffo, N. Mabnani, and G. H. Lander, *Rev. Mod. Phys.* **81**, 807 (2009).
 [2] Y. Kuramoto, H. Kusunose, and A. Kiss, *J. Phys. Soc. Jpn.* **78**, 072001 (2009).

- [3] A. S. Cameron, G. Friemel, and D. S. Inosov, *Rep. Prog. Phys.* **79**, 066502 (2016).
 [4] T. Fujita, M. Suzuki, T. Komatsubara, S. Kunii, T. Kasuya, and T. Ohtsuka, *Solid State Commun.* **35**, 569 (1980).

- [5] M. Kawakami, S. Kunii, T. Komatsubara, and T. Kasuya, *Solid State Commun.* **36**, 435 (1980).
- [6] A. Takase, K. Kojima, T. Komatsubara, and T. Kasuya, *Solid State Commun.* **36**, 461 (1980).
- [7] J. M. Effantin, P. Bulet, J. Rossat-Mignod, S. Kunii, and T. Kasuya, in *Proceedings of the International Conference on Valence Instabilities*, Zurich, edited by P. Wachter and H. Boppert (North-Holland, Amsterdam, 1982), p. 559.
- [8] O. Zaharko, P. Fischer, A. Schenck, S. Kunii, P.-J. Brown, F. Tasset, and T. Hansen, *Phys. Rev. B* **68**, 214401 (2003).
- [9] A. Schenck and G. Solt, *J. Phys.: Condens. Matter.* **16**, S4639 (2004).
- [10] K. Kunimori, M. Kotani, H. Funaki, H. Tanida, M. Sera, T. Matsumura, and F. Iga, *J. Phys. Soc. Jpn.* **80**, SA056 (2011).
- [11] K. Kunimori, M. Sera, H. Tanida, T. Matsumura, and F. Iga, *J. Phys. Soc. Jpn.* **81**, 104706 (2012).
- [12] S. Ikeda, M. Sera, S. Hane, Y. Uwatoko, M. Kosaka, and S. Kunii, *J. Phys. Soc. Jpn.* **76**, 064716 (2007).
- [13] G. Friemel, Y. Li, A. Dukhnenko, N. Shitsevalova, N. Shuchanko, A. Ivanov, V. Filipov, B. Keimer, and D. Inosov, *Nat. Commun.* **3**, 830 (2012).
- [14] H. Jang, G. Friemel, J. Ollivier, A. V. Dukhnenko, N. Y. Shitsevalova, V. B. Filipov, B. Keimer, and D. S. Inosov, *Nat. Mater.* **13**, 682 (2014).
- [15] T. Sakakibara, T. Tayama, H. Amitsuka, K. Tenya, S. Kunii, T. Suzuki, and A. Ochiai, *Physica B (Amsterdam)* **230-232**, 307 (1997).
- [16] T. Tayama, T. Sakakibara, K. Tenya, H. Amitsuka, and S. Kunii, *J. Phys. Soc. Jpn.* **66**, 2268 (1997).
- [17] M. Hiroi, M. Sera, N. Kobayashi, and S. Kunii, *Phys. Rev. B* **55**, 8339 (1997).
- [18] M. Hiroi, S. Kobayashi, M. Sera, N. Kobayashi, and S. Kunii, *J. Phys. Soc. Jpn.* **66**, 1762 (1997).
- [19] M. Hiroi, S. Kobayashi, M. Sera, N. Kobayashi, and S. Kunii, *J. Phys. Soc. Jpn.* **67**, 53 (1998).
- [20] M. Hiroi, S. Kobayashi, M. Sera, N. Kobayashi, and S. Kunii, *Phys. Rev. Lett.* **81**, 2510 (1998).
- [21] O. Suzuki, T. Goto, S. Nakamura, T. Matsumura, and S. Kunii, *J. Phys. Soc. Jpn.* **67**, 4243 (1998).
- [22] S. Kobayashi, M. Sera, M. Hiroi, N. Kobayashi, and S. Kunii, *J. Phys. Soc. Jpn.* **69**, 926 (2000).
- [23] S. Kobayashi, Y. Yoshino, S. Tsuji, H. Tou, M. Sera, and F. Iga, *J. Phys. Soc. Jpn.* **72**, 2947 (2003).
- [24] K. Kunimori, H. Tanida, T. Matsumura, M. Sera, and F. Iga, *J. Phys. Soc. Jpn.* **79**, 073703 (2010).
- [25] D. Jang, P. Y. Portnichenko, A. S. Cameron, G. Friemel, A. V. Dukhnenko, N. Y. Shitsevalova, V. B. Filipov, A. Schneidewind, A. Ivanov, D. S. Inosov, and M. Brando, *npj Quantum Mater.* **2**, 62 (2017).
- [26] S. E. Nikitin, P. Y. Portnichenko, A. V. Dukhnenko, N. Y. Shitsevalova, V. B. Filipov, Y. Qiu, J. A. Rodriguez-Rivera, J. Ollivier, and D. S. Inosov, *Phys. Rev. B* **97**, 075116 (2018).
- [27] J. C. Nickerseon and R. White, *J. Appl. Phys.* **40**, 1011 (1969).
- [28] M. Takigawa, H. Yasuoka, T. Tanaka, and Y. Ishizawa, *J. Phys. Soc. Jpn.* **52**, 728 (1983).
- [29] J. M. Effantin, J. Rossat-Mignod, P. Bulet, S. Kunii, and T. Kasuya, *J. Magn. Magn. Mater.* **47-48**, 145 (1985).
- [30] J. Rossat-Mignod, *Neutron Scattering in Condensed Matter Research*, Methods of Experimental Physics No. 23C (Academic, Orlando, 1987).
- [31] K. Hanzawa and T. Kasuya, in *Proceedings of the International Conference on High Field Magnetism*, edited by M. Date (North-Holland, Amsterdam, 1983), p. 171.
- [32] K. Hanzawa and T. Kasuya, *J. Phys. Soc. Jpn.* **53**, 1809 (1984).
- [33] Y. Y. Hsieh and M. Blume, *Phys. Rev. B* **6**, 2684 (1972).
- [34] T. M. Holden, E. C. Svensson, W. J. L. Buyers, and O. Vogt, *Phys. Rev. B* **10**, 3864 (1974).
- [35] M. Kohgi, K. Iwasa, M. Nakajima, N. Metoki, S. Araki, N. Bernhofft, J.-M. Mignot, A. Gukasov, H. Sato, Y. Aoki, and H. Sugawara, *J. Phys. Soc. Jpn.* **72**, 1002 (2003).
- [36] R. Shiina, *J. Phys. Soc. Jpn.* **73**, 2257 (2004).
- [37] E. Zirngiebl, B. Hillebrands, S. Blumenröder, G. Güntherodt, M. Loewenhaupt, J. M. Carpenter, K. Winzer, and Z. Fisk, *Phys. Rev. B* **30**, 4052(R) (1984).
- [38] B. Luthi, S. Blumenroder, B. Hillebrands, E. Zirngieble, G. Guntherodt, and K. Winzer, *Z. Phys. B* **58**, 31 (1984).
- [39] F. J. Ohkawa, *J. Phys. Soc. Jpn.* **52**, 3897 (1983).
- [40] F. J. Ohkawa, *J. Phys. Soc. Jpn.* **54**, 3909 (1984).
- [41] R. Shiina, H. Shiba, and P. Thalmeier, *J. Phys. Soc. Jpn.* **66**, 1714 (1997).
- [42] H. Shiba, O. Sakai, and R. Shiina, *J. Phys. Soc. Jpn.* **68**, 1988 (1999).
- [43] W. A. C. Erkelens, L. P. Renault, P. Bulet, J. Rossat-Mignod, S. Kunii, and T. Kasuya, *J. Magn. Magn. Mater.* **63**, 61 (1987).
- [44] O. Sakai, R. Shiina, H. Shiba, and P. Thalmeier, *J. Phys. Soc. Jpn.* **66**, 3005 (1997).
- [45] R. Shiina, O. Sakai, H. Shiba, and P. Thalmeier, *J. Phys. Soc. Jpn.* **67**, 941 (1998).
- [46] H. Nakao, K. Magishi, Y. Wakabayashi, Y. Murakami, K. Koyama, K. Hirota, Y. Endoh, and S. Kunii, *J. Phys. Soc. Jpn.* **70**, 1857 (2001).
- [47] T. Matsumura, T. Yonemura, K. Kunimori, M. Sera, and F. Iga, *Phys. Rev. Lett.* **103**, 017203 (2009).
- [48] M. Sera and S. Kobayashi, *J. Phys. Soc. Jpn.* **68**, 1664 (1999).
- [49] M. Sera, *J. Phys. Soc. Jpn.* **69**, 2299 (2000).
- [50] M. Sera, H. Ichikawa, T. Yokoo, J. Akimitsu, M. Nishi, K. Kakurai, and S. Kunii, *Phys. Rev. Lett.* **86**, 1578 (2001).
- [51] S. Kobayashi, M. Sera, M. Hiroi, N. Kobayashi, and S. Kunii, *J. Phys. Soc. Jpn.* **68**, 3407 (1999).
- [52] G. Uimin, Y. Kuramoto, and N. Fukushima, *Solid State Commun.* **97**, 595 (1996).
- [53] N. Fukushima and Y. Kuramoto, *J. Phys. Soc. Jpn.* **67**, 2460 (1998).
- [54] K. Hanzawa, *J. Phys. Soc. Jpn.* **70**, 468 (2001).
- [55] R. Shiina, *J. Phys. Soc. Jpn.* **70**, 2746 (2001).
- [56] K. Magishi, M. Kawakami, T. Saito, K. Koyama, K. Mizuno, and S. Kunii, *Z. Naturforsch. A* **57**, 441 (2002).
- [57] H. Takagiwa, K. Ohishi, J. Akimitsu, W. Higemoto, R. Kadono, M. Sera, and S. Kunii, *J. Phys. Soc. Jpn.* **71**, 31 (2002).
- [58] K. Iwasa, K. Kuwahara, M. Kohgi, P. Fisher, A. Donni, L. Keller, T. Hansen, S. Kunii, N. Metoki, Y. Koike, and K. Ohoyama, *Physica B (Amsterdam)* **329-333**, 582 (2003).
- [59] P. Fischer, K. Iwasa, K. Kuwahara, M. Kohgi, T. Hansen, and S. Kunii, *Phys. Rev. B* **72**, 014414 (2005).
- [60] A. Schenck, F. N. Gyax, and G. Solt, *Phys. Rev. B* **75**, 024428 (2007).
- [61] K. Kubo and Y. Kuramoto, *J. Phys. Soc. Jpn.* **72**, 1859 (2003).
- [62] K. Kubo and Y. Kuramoto, *J. Phys. Soc. Jpn.* **73**, 216 (2004).

- [63] D. Mannix, Y. Tanaka, D. Carbone, N. Bernhoeft, and S. Kunii, *Phys. Rev. Lett.* **95**, 117206 (2005).
- [64] K. Kuwahara, K. Iwasa, M. Kohgi, N. Aso, M. Sera, and F. Iga, *J. Phys. Soc. Jpn.* **76**, 093702 (2007).
- [65] T. Matsumura, S. Michimura, T. Inami, T. Otsubo, H. Tanida, F. Iga, and M. Sera, *Phys. Rev. B* **89**, 014422 (2014).
- [66] T. Inami, S. Michimura, Y. Hayashi, T. Matsumura, M. Sera, and F. Iga, *Phys. Rev. B* **90**, 041108(R) (2014).
- [67] A. Kondo, H. Tou, M. Sera, and F. Iga, *J. Phys. Soc. Jpn.* **76**, 013701 (2007).
- [68] T. Goto, A. Tamaki, T. Fujimura, N. Sato, S. Kunii, and T. Kasuya, *J. Magn. Magn. Mater.* **52**, 253 (1985).
- [69] M. Sera, N. Sato, and T. Kasuya, *J. Magn. Magn. Mater.* **63 & 64**, 64 (1987).
- [70] M. Sera, N. Sato, and T. Kasuya, *J. Phys. Soc. Jpn.* **57**, 1412 (1988).